AD-760 578

AN EXPERIMENTAL STUDY OF THE EROSION REBOUND CHARACTERISTICS OF HIGH SPEED PARTICLES IMPACTING A STATIONARY SPECIMEN

G. Grant, et al

Cincinnati University

Prepared for:

Army Research Office-Durham

May 1973

REPORT NO. 73-36

Department of Aerospace Engineering
University of Cincinnati

AN EXPERIMENTAL STUDY OF THE EROSION REBOUND CHARACTERISTICS OF HIGH SPEED PARTICLES IMPACTING A STATIONARY SPECIMEN

G. Grant, R. Ball, and W. Tabakoff

May 1973

This work was supported by the U.S. Army Research Office - Durham under Grant Number DA-ARO-D-124-G-154.

REPORT NO. 73-36

AN EXPERIMENTAL STUDY OF THE EROSION REBOUND CHARACTERISTICS OF HIGH SPEED PARTICLES IMPACTING A STATIONARY SPECIMEN

G. Grant, R. Ball, and W. Tabakoff

May 1973

This work was supported by the U.S. Army Research Office - Durham under Grant Number DA-ARO-D-124-G-154.

TABLE OF CONTENTS

LIST OF ILLUSTRATIONS

Unclassified
Security Classification

DOCUMENT CONTROL DATA - R & D

(Security classification of title, body of abstract and indexing annotation must be entered when the overall report is classified)

1. ORIGINATING ACTIVITY *(Corporate author)*

University of Cincinnati

2a. REPORT SECURITY CLASSIFICATION

Unclassified

2b. GROUP

N/A

3. REPORT TITLE

An Experimental Study of the Erosion Rebound Characteristics of High Speed Particles Impacting a Stationary Specimen

4. DESCRIPTIVE NOTES *(Type of report and inclusive dates)*

Technical Report

5. AUTHOR(S) *(First name, middle initial, last name)*

G. Grant, R. Ball, and W. Tabakoff

6. REPORT DATE	7a. TOTAL NO. OF PAGES	7b. NO. OF REFS
May 1973	35 45	14

8a. GRANT NO.	9a. ORIGINATOR'S REPORT NUMBER(S)
DA-ARO-D-124-G-154	Report No. 73-36
b. PROJECT NO. 31 71	
c.	9b. OTHER REPORT NO(S) *(Any other numbers that may be assigned this report)*
d.	

10. DISTRIBUTION STATEMENT

Distribution of this report is unlimited

11. SUPPLEMENTARY NOTES	12. SPONSORING MILITARY ACTIVITY
None	U.S. Army Research Office-Durham Box CM, Duke Station Durham, North Carolina 27706

13. ABSTRACT

The impact and rebound characteristics of high speed solid particles have been experimentally determined. This study was limited to a system where the particle material is much harder than the target material and thus erosion takes place at impact. The impact parameters were found to be statistical in nature and thus the statistical distributions were obtained. The effect of the particle velocity and impact angle was also investigated. In addition, the rebound data was related to the erosion damage.

Key Words:

Erosion

DD FORM 1473 REPLACES DD FORM 1473, 1 JAN 68, WHICH IS OBSOLETE FOR ARMY USE.

Unclassified
Security Classification

NOMENCLATURE

Symbol	
E	Quantity of erosion (mgms)
M	Mass
RR	Ratio of conditions after impact to those before impact (Restitution Ratio)
V	Particle velocity
W	Quantity of mass eroded
β	Relative angle between particle path and specimen
ε	Erosion rate
α	Power of velocity that erosion is proportional ($\varepsilon \sim V^{\alpha}$)
ϕ	Kinetic energy required to erode one unit mass of material at small angles of attack
σ	Standard deviation of a normal distribution

Subscripts	
1	Approach conditions
2	Rebound conditions
n	Component normal to specimen surface
t	Component tangent to specimen surface

INTRODUCTION

The erosion of metals by particulate flows has been the subject of numerous investigations spanning the last two decades. The study of erosion has been of great importance in such diverse industries as oil processing, transportation and rocketry. Recent interest into this old problem coincides with the increased usage of gas turbines in dusty environments. This is primarily a result of the stepped up employment of the helicopter, which has the inherent ability to land on unprepared or dusty terrains.

The problem of predicting erosion in gas turbines and compressors is extremely complex and has not been satisfactorily discussed in the literature. The complexity is primarily a result of the fact that the particle trajectory must be traced through the flow field after multiple impacts. When a sand particle collides with a high speed rotor, the erosion can be predicted in a conventional manner if coordinates relative to the rotor are chosen. However, after impacting the rotor and causing the subsequent erosion, the sand particle will rebound with an even higher velocity with respect to the stator and will cause serious damage to it. Further, the particle dynamics resulting from these impacts cause the contaminant particle to centrifuge to the blade tips where the localized high concentration causes severe damage to a very vulnerable region. This damage, of course, will result in the loss of performance, and in the case of a compressor, a decrease in stall margine.

In general, the impact dynamics of erosive particles have been overlooked. Without this knowledge the erosion of systems, such as rotating machinery, where a multiplicity of impacts take place, cannot be adequately modeled. The changes in particle velocity can best be measured by a quantity known as the restitution coefficient, which is defined as the ratio of particle velocity after impact to the particle velocity before impact. The change in the velocity of these erosive particles involves a direction as well as a magnitude. For this reason, the ratio of the components of velocity normal to the specimen surface and tangent to the surface were included.

STATE OF THE ART

A survey of the literature concerning restitution coefficients yielded little information on the problem being investigated. The restitution ratio is a measure of the kinetic energy exchange upon impact. It is therefore important that the coefficient used in a system undergoing erosion adequately represent the physical energy exchange mechanism. Erosion is normally defined as the removal of surface material by a stream of solid particles. For the purposes of this paper it takes place when the contaminant particle is much harder than the target material. Thus, the energy exchange mechanism is one of target distortion rather than the distortion of the particle. Further, since the scope of this report is limited to ductile

materials, the particle will create local stresses high enough to cause plastic flow of the target material. With this in mind, a survey of the literature concerning restitution coefficients was undertaken.

One of the earliest discussions of particle restitution ratios was given by Tabor (1) where he discussed the hardness of metals. In his analysis he equated the volume of the indentation to the loss of kinetic energy of the indenter (restitution ratio). Tabor gathered data on the rebounding characteristics of a spherical indenter using a Shore Rebound scleroscope and compared this data to a theoretical model which he developed. This theoretical model was arrived at by making the following assumptions:

(i) The particle is spherical.

(ii) The angle of impact is 90^{o}.

(iii) The particle absorbs no energy due to deformation.

(iv) The local stress at impact can be predicted by Hertz's equations.

(v) The dynamic yield pressure is constant when the condition of plastic flow is reached.

Using his analysis, Tabor came to the conclusion that the velocities before and after impact were not linearly related and therefore the restitution ratio was not constant for the range of velocities investigated. At very low velocities (depending on the material tested) the impacts were essentially elastic and the restitution ratio was equal to one. As the magnitude of velocity was increased, the restitution ratio seemed to approach a constant independent of the approach velocity. Tabor's analysis is important both from a historical standpoint and due to the fundamental approach he took, however, his analysis was only carried out for very low velocities (less than 30 ft/sec) and verified experimentally for even lower velocities (less than 20 ft/sec). This is well below the erosion threshold and thus it is expected that the mechanism will be different for high speed particles.

The rebound characteristics of particles with a velocity fast enough to cause erosion were reported by Head (2). His research was principally involved with erosion of materials and to adequately model his results it was necessary to know the particle velocities before the impact. To accomplish this he took double exposed photographs of the particles using a stroboscopic light source. Further, he found that he could measure the particle velocity after impact by relocating the camera. Unfortunately, with this method it is impossible to find the velocity of the same particle before and after impact. To account for this Head took numerous pictures and from his reduced data he defined the restitution ratio as the maximum observed velocity after impact divided by the maximum observed velocity before impact. From the data reported herein, it will be shown that the maximum rebound velocity will not necessarily result from the maximum inbound velocity, and in fact, the restitution ratio can only be described as a statistical function. Head further noted

that the reliability of the data was not good due to the positioning of the camera and only major trends in the data could be estimated. However, he did conclude that the restitution ratio is independent of particle size.

Hussein and Tabakoff (3) investigated the impact and rebound phenomena of particles in a two dimensional cascade using high speed photography. This paper reported on the particle velocity restitution coefficient, as well as the restitution coefficient of the normal and tangential components of velocity. Further, they obtained data on the ratio of the particle reflection angle to the particle incidence angle which is referred to as the directional coefficient in this report.

The projectiles used in the investigation of Reference 3 were 300, 1000 and 2000 micron particles of corn cob impacting on stainless steel. From the results of their investigation, the authors concluded that the restitution ratios and directional coefficients are only a function of the angle of incidence and hence these ratios are independent of the magnitude of the oncoming particle velocity and/or of the particle diameter. These authors' curve fitted their data and obtained the following expressions.

$$\frac{V_{t_2}}{V_{t_1}} = 0.95 + 0.00055\ \beta_1 \tag{1}$$

$$\frac{V_{n_2}}{V_{n_1}} = 1.0 - 0.02108\ \beta_1 + 0.0001417\ \beta_1^2 \tag{2}$$

$$\frac{\beta_2}{\beta_1} = \frac{1}{\beta_1} \cdot \cot^{-1}\left[\left(\frac{V_{t_2}}{V_{t_1}} \cdot \frac{V_{n_1}}{V_{n_2}}\right) \cdot \cot \beta_1\right] \tag{3}$$

$$\frac{V_2}{V_1} = \frac{V_{n_2}}{V_{n_1}} \cdot \sqrt{\frac{1 + \cot^2 \beta_2}{1 + \cot^2 \beta_1}} \tag{4}$$

where β is in degrees.

The difficulty in drawing conclusions from Reference (3) comes from the fact that the particle material used in the investigation (corn cobs) is not an erosive material. In this case the particles in the airstream are much softer than the target specimen and the restitution ratio is a measure of the energy dissipated due to the distortion of the particle upon impact rather than the distortion of material. In the study of eroding systems just the opposite is true.

The restitution coefficient is a measure of the work that the particle transmits to the target material. This work results in a slight amount of material moving on the target specimen until a portion of this material actually leaves the surface and results in erosion. Thus, it is not expected that these results would apply to the system under consideration.

In general, one would expect the restitution ratio to correlate with the erosion data in that the kinetic energy lost by the particle is absorbed by target material. Neilson and Gilchrist (4) proposed that ϕ units of kinetic energy must be absorbed by a surface to release one unit mass of eroded material at small angles of attack. Their equation for erosion was expressed as the following relationship.

$$E = \frac{\frac{1}{2} M(V_1^2 \cos^2 \beta_1 - V_2^2 \cos^2 \beta_2)}{\phi} \tag{5}$$

where E is the erosion produced by M poinds of particles at an angle of attack of β_1 and particle velocity V_1. By using the tangential restitution coefficient, which is defined as:

$$RR_T = \frac{V_2 \cos \beta_2}{V_1 \cos \beta_1} \tag{6}$$

and substituting into Equation (5) gives the quantity of mass eroded:

$$E = \frac{\frac{1}{2} M V^2 \cos^2 \beta_1 (1 - RR_T^2)}{\phi} \tag{7}$$

The figure below depicts the relationship between angle of attack and material weight loss due to eroding a ductile specimen at constant particle velocity.

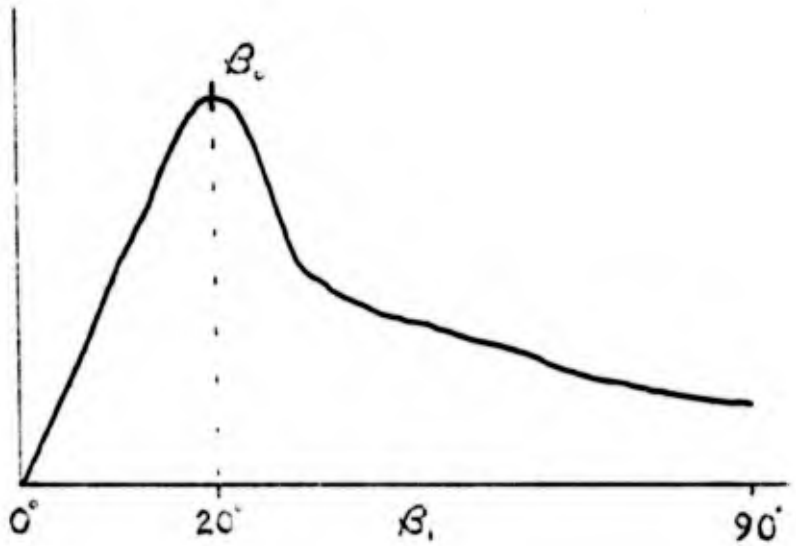

Basically, Equation (7) is an energy balance equating the energy lost by the particle at small impact angles to the material removed from the surface.

EXPERIMENTAL METHOD

Photographic Method

The standard test device for determining particle velocities was first described by Finnie (5). This system measured the particle velocity by taking double exposed pictures of a particle using a stroboscopic light source. Everytime the light pulses go on, the camera recorded the location of the particle. By measuring the distance the particle travels between the timed light pulses, the velocity of the particle is calculated. This technique has satisfied the needs of most researchers, and has thus become the standard test device for determining particle velocities.

For the research being reported it was decided to use high speed photography as a means of particle flow visualization. The development of this technique was difficult in that no literature could be found concerning the problem and a certain amount of trial and error development work was necessary. However, the method was chosen as it allowed a large number of data points to be taken at almost the same time, thus keeping the conditions of flow constant and enabling an accurate assessment of the particle environment to be made.

The camera used to photograph the particles was a 16mm Hycam camera with a one-half framer, enabling 22,000 half frames per second to be produced at top speed. The pictures were taken on 400 foot rolls of 4x Reversal Kodak high speed film using two Sylvania FF-33 flood flash lamps as a source of light. The particle was recorded on the film as a result of backscatter of light off of it, thus it was important that a very dark, nonreflecting background be used. To accomplish this the back of the test section was painted using Nextel Brand Velvet Coating (101-C10 Black) produced by the 3M Company.

Test Facility

A specially designed wind tunnel was constructed to conduct this research. A detailed description with illustrations of this facility are found in Reference (6). The main considerations in designing the test equipment were controlling the primary variables of fluid velocity, particle velocity, particle flow rate and particle sizes in a representative aerodynamic environment. Provisions are designed into the tester to vary the angle of attack between the abrasive particle and the surface of the test specimen.

Figure 1 is a schematic of the apparatus which fulfills these objectives. As depicted in this illustration, the equipment functions as follows.

A measured amount of abrasive grit of a given consistency is placed into the particle feeder A. The particles are fed into a secondary air source and blown up to the particle injector, C, where it mixes with the main air supply, B. The particles are then accelerated by the high velocity air in a constant area duct, D, and impact the specimen in the test section, E. The test dust is then separated from the air by a cyclone separator, G, and collected in a container, H. The test air is then further filtered through a commerical 5μ filter, F.

The test section was designed such that the experiments can be run in a rapid manner without destroying the aerodynamic parameters. The basic geometry of the test section is illustrated on Figure 2. From this figure it can be seen that the tunnel geometry is uninterupted from the acceleration tunnel into the test section. In this manner the particle laden air is channeled over the specimen and the aerodynamics of the fluid passing over the blade at the given angle of attack are preserved. In order to minimize the tunnel blockage, three sized specimens were used. At angles of attack of 0 to 20 degrees a one inch wide specimen was used, from 20 to 45 degrees, a one-half inch wide specimen is used and for the large angles of attack of 45 to 90 degrees, a one-fourth inch wide specimen was used. In this manner, the maximum tunnel blockage is on the order of 10%.

The test section was constructed with several different inserts to obtain all of the required data. Figure 2 illustrates the basic test section geometry and the test specimen holder. The channel geometry is the same as that of the acceleration section, that is 3 inches x 1 inch, up to the location of the specimen where the channel turns 30 degrees. Figure 3 illustrates the photographic insert through which high speed photography and streak photographs were taken of the erosive sand particles. This insert consists of an enclosure plate, a replaceable glass insert and a collar to hold the insert in. The high speed particles scratch the glass through which the pictures are taken through, thus this insert is replaced after each test. This unique test facility has resulted in very high quality pictures without disrupting the flow field.

Analysis of the Photographic Data

Two techniques of analysis were used in reducing the photographic data. These procedures are complimentary in that one was used to check the other. Both of these methods relied on a reference distance which was marked on the test section background. The particle velocities were obtained by comparing the distance traveled by the particle in two successive frames to this reference distance. The following discussion is based on the illustration and nomenclature of Figure 4.

The first method of analysis is essentially one of streak photography. The velocity is determined by dividing the distance traveled by the particle during the exposure time for one frame.

The velocity is calculated using the equation

$$V = (L \frac{r}{R})/t_e \quad (8)$$

where

V - Particle velocity (ft/sec)

L - Length of particle streak on screen (ft)

r - Actual length of reference line (ft)

R - Reference line projected on screen (ft)

t_e - Exposure time of frame observed (sec)

The second method of analysis was based on the distance a particle travels in successive frames. The basic concept is the same as the first method, however, it was found to give more accurate results. The particle velocity is determined using the equation,

$$V = m \frac{r}{R} S \quad (9)$$

where

m - Length traveled by particle between two successive frames (ft)

S - Film speed (local quantity) (ft/sec)

r and R are the same as in Equation (8).

In practice a combination of the two methods was used and checked against each other.

EXPERIMENTAL RESULTS AND DISCUSSION

The erosion of metals impacted by small dust particles as well as the rebound dynamics of these particles can only be described in a statistical sense. This becomes obvious when one examines the number of geometric situations that might occur at impact. After a given incubation period, the target material will become pitted with craters and in fact after a slightly longer time period, a regular ripple pattern may form on the eroded surface (7). Thus the local impact angle between the small particle and the eroded surface may deviate considerably from the geometric average. Further, the particles themselves are irregular crystalline in shape with several sharp corners. As the particle approaches the specimen the orientation of the particle is, for the most part, random. Thus, some particles will impact on a flat surface and do very little work on the target material. Others will impact with a

corner oriented in a manner where it will remove material in a method similar to that of a cutting tool. This effect of particle orientation on erosion has been discussed in the literature (8,9).

The statistical study required a somewhat lengthy analysis due to the large number of impacts that were examined. This fact limited the number of cases that were tested. The final test program consisted of four tests which examined the effect of angle of attack as well as particle velocity. Variables that could be of importance but not analyzed were particle material, target material, and particle size. Quartz sand was picked due to its high reflective qualities. Alumina sand was tried but the photographic results were not of sufficient quality to be used. The target material used for this pilot study was annealed 2024 aluminum alloy. This material was chosen due to the large amount of erosion test data available on it in the literature. Tests using other materials will be performed in the near future. The particle size used for this test was 200μ. The experimental variables studied are described in Table I.

The statistical data is presented using histograms to best describe the distribution of the data. Figure 5, illustrates the histogram of the velocity restitution ratio, at an angle of attack of 20 degrees. As can be seen from this figure, the data is presented by a series of rectangles. The height of the rectangle, or frequency of occurrence, represents the number of times that velocity restitution ratio was observed to be between the limits designated by the base of the rectangle. The mean, or average value of the parameter, is also marked on the graph. Thus, this one figure illustrates the complete nature of the data.

The velocity information (both magnitude and direction) was obtained in a manner described earlier. Figures 5, 6 and 7 illustrate the statistical distributions of the velocity ratio (V_2/V_1) at angles of attack of 20, 45 and 90 degrees, respectively, and a particle velocity of 250 feet per second. This data indicates V_2/V_1 drops continuously as β_1 is increased. At 20 and 45 degrees the distribution is wider than at 90 degrees, further the data appears to be slightly skewed in the direction of higher V_2/V_1.

On Figure 8 the data is summarized. The solid line represents the least squares polynomial curve fit of the average values from Figures 5, 6 and 7. Further, the shape of the distributions are cross plotted on this figure. Thus, the influence of β_1 on V_2/V_1 can be seen at a glance.

The parameter V_2/V_1 is directly related to the kinetic energy lost during impact. The spread in this data indicates the variable condition of the surfaces and the orientation of the particle at impact. For the system tested it appears that glancing blows are more efficient in rebounding than direct impacts since V_2/V_1 increases with decreasing β_1. This is very interesting since just the opposite is true for erosion, viz, erosion at low angles of attack is greater than that at high angles of attack. Some researchers (2) have developed models which relate the erosion loss

directly to the kinetic energy loss. These results would indicate that just the opposite is true.

With these unexpected results it was decided to continue the investigation and examine the manner that the directional coefficient β_2/β_1 changes with β_1. Again, the data was plotted in the form of histogram. Figure 9 illustrates the histogram of this data when β_1 equals 20 degrees. The spread of this parameter on Figure 9 varies from zero to two. A ratio of one would indicate that the normal and tangential components of V_1 are reduced by the same ratio. Thus, it would appear that almost any value of β_2/β_1 is possible at this angle. Figures 10 and 11 illustrate the histograms of this parameter at angles of attack of 45 and 90 degrees, respectively. This data appears to have a better defined distribution, however, the spread of observed values is still extremely high at 90 degrees. (It must be remembered that the distribution of V_2/V_1 was very small at 90 degrees). On Figure 12 the data is again summarized as before. Viewing the data in this manner the statistical variation is dramatically apparent. At 20 degrees the statistical data spreads all over the page yet at an angle of attack of 45 degrees the data appears to have a normal, bell shaped distribution. Finally, at normal impact the data spreads out again, but not as dramatically as was the case at 20 degrees.

The spread of the distribution of β_2/β_1 can most likely be directly linked to the condition of the target surface at that value of β_1. In viewing the same specimens after impact, at small values of β_1, a regular ripple pattern could be seen forming on the material. These ripples cause the surface of the specimen to vary sinusoidally in a manner that changes the local impact angle considerably (7). This then is no doubt the cause of the wide dispursion of the data as seen on Figure 9. At 45 degrees β_1, the ripple mechanism ceases and the normal distribution again appears as is seen on Figure 10. The most interesting results of all are those obtained at 90 degrees or normal impact. As these particles approach the plate, they have no component of velocity parallel to it. However, the mean of the direction coefficient at this angle is 0.683, thus, the particles are turned an average of 28.5 degrees after impacting this supposedly flat surface. A close check of the movies indicated that this phenomena was independent of the location of impact on the specimen, such that aerodynamic effects can be discounted. The most probable reason for this process is again the irregularity of the specimen surface. The significance of this data is that it explains why ductile erosion occurs at 90 degrees where many theories of erosion predict that no erosion will occur at this angle (8).

Since the directional coefficient gave such complicated results it was decided to break the velocity vector down into its normal and tangential components and investigate these independently. Figure 13 illustrates a histogram of the ratio of the normal component of the velocity vector before and after impact at an angle of attack of 20 degrees. As was the case with the directional coefficient, the spread in this data is such that almost anything is possible. The possible results range from a complete loss of the normal velocity component to a normal component higher than the value before impact. Figures 14

and 15 illustrate the histograms of this parameter as β_1 is increased to 45 and 90 degrees. This data shows the same trend as the total vector ratio V_2/V_1, i.e., the restitution ratio decreased with increasing angle of attack. This trend is illustrated on Figure 16 where again the average value of the parameter is plotted as a solid line and the distributions are overlayed onto the plot.

Figures 17 and 18 illustrate the histograms for the ratio of the tangential component of velocity, V_{T_2}/V_{T_1} at angles of attack of 20 and 45 degrees. The data for 90 degrees is not presented as this parameter is undefined at this point. On Figure 19 where the data is summarized, the tangential restitution ratio was assumed to be unity at 90 degrees. The average values of V_{T_2}/V_{T_1}, plotted on Figure 19, are the only data analyzed which support the theory that erosion is proportional to a particle kinetic energy loss at impact. The maximum erosion of the material tested (2024 aluminum) occurs at β_1 of 20 degrees. This is also where the V_{T_2}/V_{T_1} reaches a minimum.

These results indicate that the normal component of velocity does not significantly contribute to ductile erosion. Most probably the kinetic energy is dissipated by plastic deformation of the target material without significant material removal. On the other hand, the loss of the tangential component of the particle velocity at impact does correlate with the erosion results. These facts support the model of erosion proposed by Finnie (8).

The solid lines on Figures 8, 12, 14, and 19 represent a least squares polynomial curve fit of the mean value of the restitution parameter and may be expressed by the equations:

$$V_2/V_1 = 1.0 - 2.03\ \beta_1 + 3.32\ \beta_1^2 - 2.24\ \beta_1^3 + 0.472\ \beta_1^4$$

$$\beta_2/\beta_1 = 1.0 + 0.409\ \beta_1 - 2.52\ \beta_1^2 + 2.19\ \beta_1^3 - 0.531\ \beta_1^4$$

$$V_{n_2}/V_{n_1} = 0.993 - 1.76\ \beta_1 + 1.56\ \beta_1^2 - 0.49\ \beta_1^3$$

$$V_{t_2}/V_{t_1} = 0.938 - 1.66\ \beta_1 + 2.11\ \beta_1^2 - 0.67\ \beta_1^3$$

For a comparison of the erosive and nonerosive results, the general equations of restitution coefficients from Reference 3 have been plotted on Figures 8, 12, 14 and 19 using a dashed line. Although one would not necessarily expect this data to agree, it is very interesting to note how well the rebound coefficient for the normal component of velocity do in fact correlate.

Equations for the standard deviation of the normal and tangential velocity restitution ratio were also obtained so that the effect of impact angle on the statistical behavior of these parameters could be further examined. The total velocity restitution

coefficient (V_2/V_1) and the directional coefficient (β_2/β_1) were not examined as their distributions did not appear to be normal. The equations for the examined parameters are as follows.

$$\sigma(V_{T_2}/V_{T_1}) = -0.0005 + 0.62\ \beta_1 - 0.535\ \beta_1^2 + 0.089\ \beta_1^3$$

$$\sigma(V_{N_2}/V_{N_1}) = 2.15\ \beta_1 - 5.02\ \beta_1^2 + 4.05\ \beta_1^3 - 1.085\ \beta_1^4$$

where σ is standard deviation of the normal distribution.

Figures 20, 21, 22, and 23 illustrate the four restitution ratio parameters in question at higher velocity (390 ft/sec) and 45 degree angle of attack. These distributions have the same form as those observed at the lower velocity (250 ft/sec) and 45 degrees illustrated on Figures 6, 10, 14, and 18. The similarity of the shape of the distribution can be further exemplified by reviewing the standard deviations of the equivalent parameters listed on Table I. This fact is very important as it illustrates the reproducibility of the statistical data.

Figure 24 illustrates the average or mean values of the restitution ratio parameters against velocity. Since only two different velocities were tested it was felt that the specific results should not be overly stressed, however, the general trends should be noted. It has been pointed out previously in this report that all other authors have assumed the restitution ratio to be invarient to the magnitude of the approach velocity (after an initial incubation velocity of a few feet per second). However it can be seen on Figure 19, or the data presented in Table I, that this is not necessarily so. In particular the tangential restitution ratio appears to be very susceptible to the magnitude of approach velocity. This fact is especially important in that it is this parameter that most influences the erosion rate of the target material.

The effect of particle velocity, V, on the erosion rate, ε, has been investigated by a number of authors (6,8-12). Most of the results have been depicted by a simple power relationship, i.e.,

$$\varepsilon = KV^{\alpha}$$

Typical values of the velocity exponent, α, range between 2.3 and 2.9. These results seem to contradict the theory based on kinetic energy that this exponent equal 2. The higher experimental values of α have bothered some authors, and several explanations have been proposed (10,13,14). However, since it has been determined that the tangential restitution ratio is indeed a function of the particle velocity, it is felt that the experimental study of this parameter may verify or disprove these conclusions.

CONCLUSIONS

The dynamic impact characteristics of erosive particles impacting a ductile material with resulting erosion have been experimentally investigated. The results of this investigation have led to the following conclusions.

1. The kinetic energy lost by the particle can be expressed in terms of restitution coefficients. In theory, this parameter should then be proportional to the resulting erosion.

2. The characteristics of an eroding system are problematic and must be defined statistically.

3. The tangential component of the velocity restitution ratio correlates with the experimentally observed erosion results, whereas the normal component of this parameter exhibits no such correlation.

4. The particles impacting the specimen at right angles rebound at oblique angles in most cases due to the irregular surface. This could explain the erosion resulting from normal impact.

5. The restitution ratio decreases as the particle impact velocity increases.

It is felt that these data provide a new insight into the erosion phenomena as well as to provide the basic data required for trajectory analysis where multiple impacts take place.

TABLE I

Summary of Results

Target Material - 2024 Aluminum Alloy

Particle Material - Silica Sand (Quartz)

Particle Size - 200μ

Restitution Ratio Parameter	Incoming Angle of Attack	Incoming Particle Velocity	Sample Statistical Mean	Standard Deviation	Sample Size (#)
Velocity V_2/V_1	20°	250 ft/sec	.607	.1503	207
	45°	250	.550	.1445	121
	45°	390	.400	.1469	177
	90°	250	.210	.0655	253
V_{n_2}/V_{n_1}	20°	250	.525	.2941	207
	45°	250	.362	.1367	121
	45°	390	.334	.1391	177
	90°	250	.176	.0616	253
V_{t_2}/V_{t_1}	20°	250	.600	.1529	207
	45°	250	.717	.2019	121
	45°	390	.654	.2220	177
	90°	250	-	-	253
β_2/β_1	20°	250	.921		207
	45°	250	.626		121
	45°	390	.633		177
	90°	250	.683		253

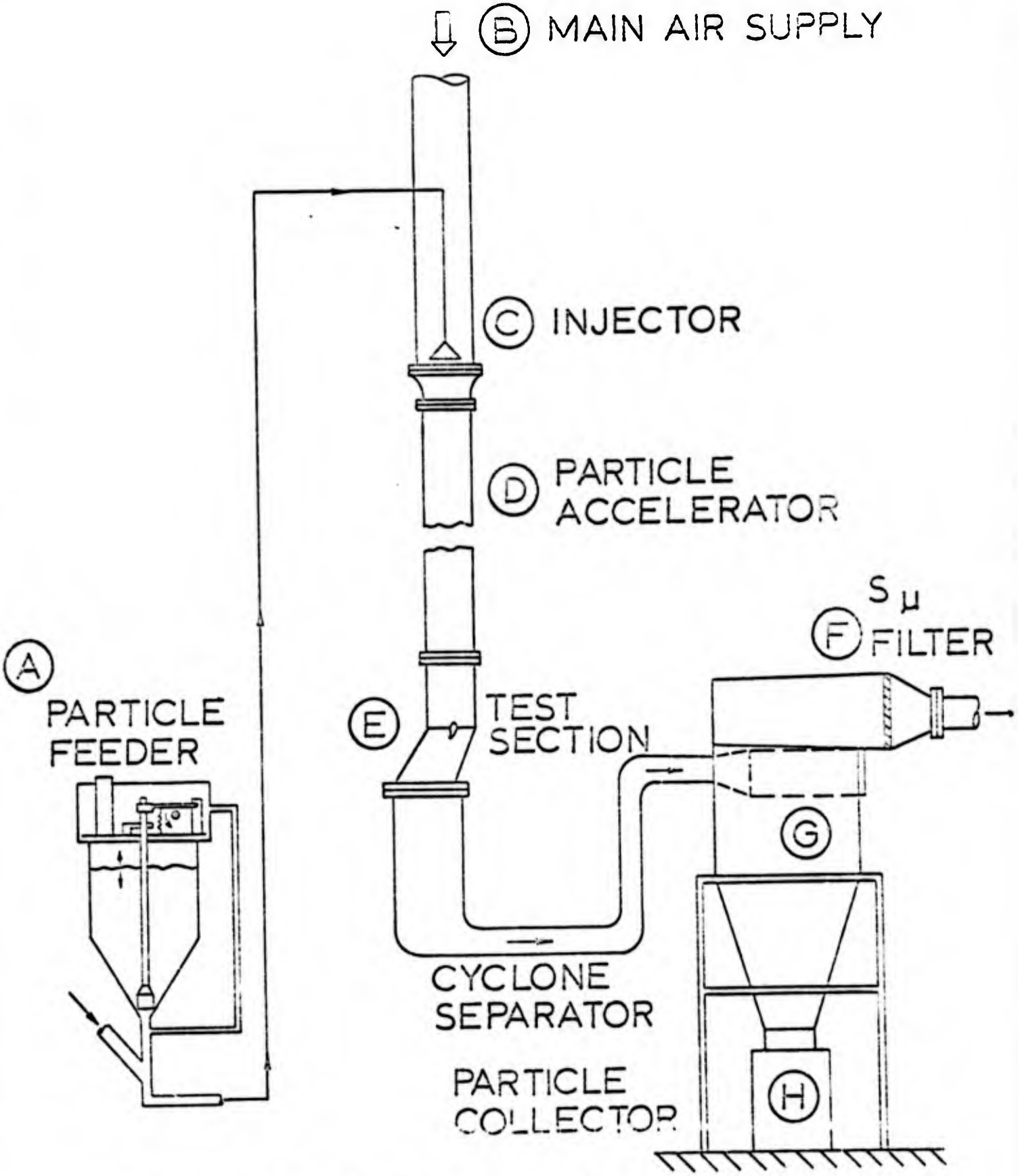

FIG. 1 EROSION TEST SCHEMATIC
EROSION RESEARCH FACILITY

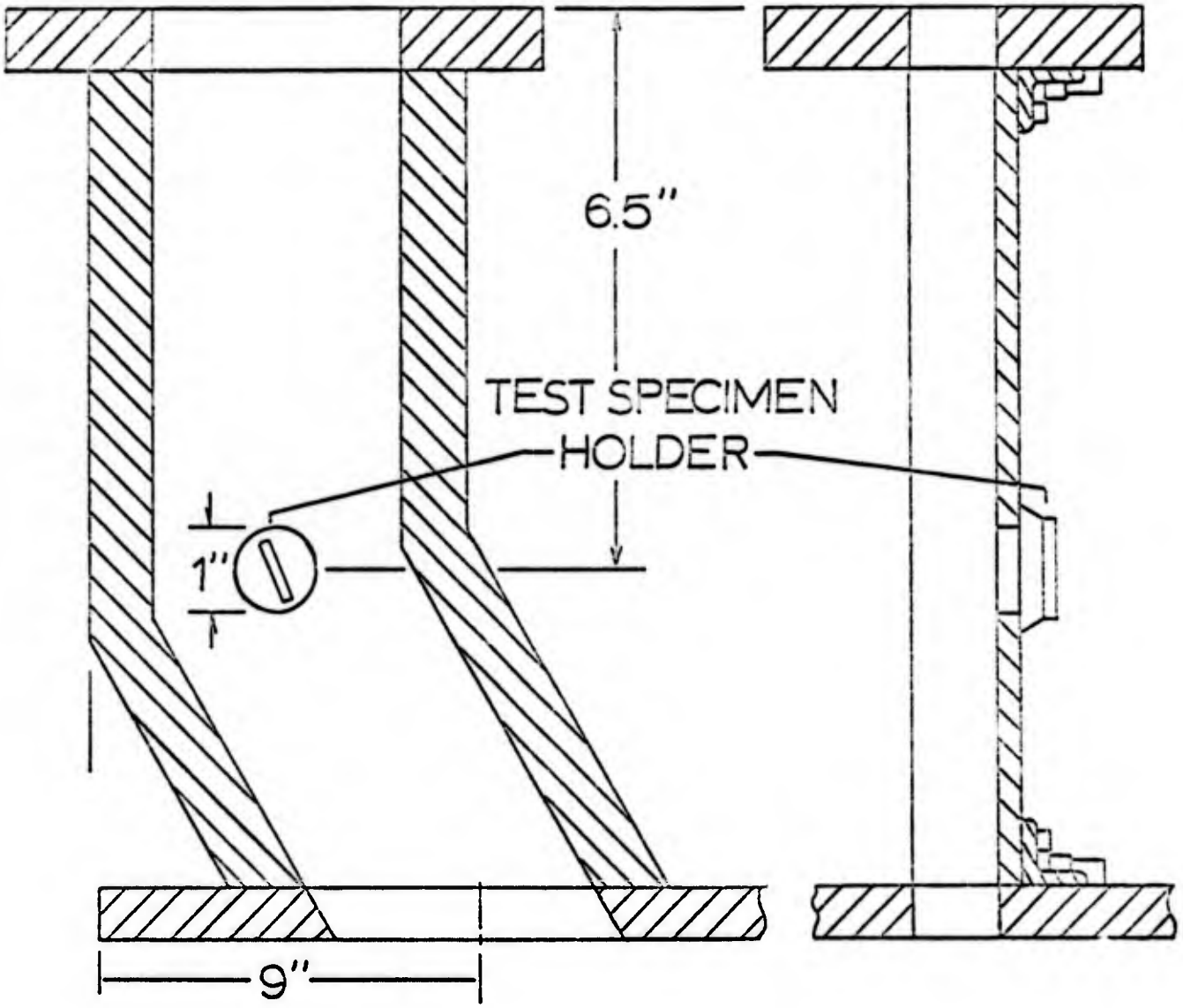

FIG. 2 TEST SECTION

EROSION RESEARCH FACILITY

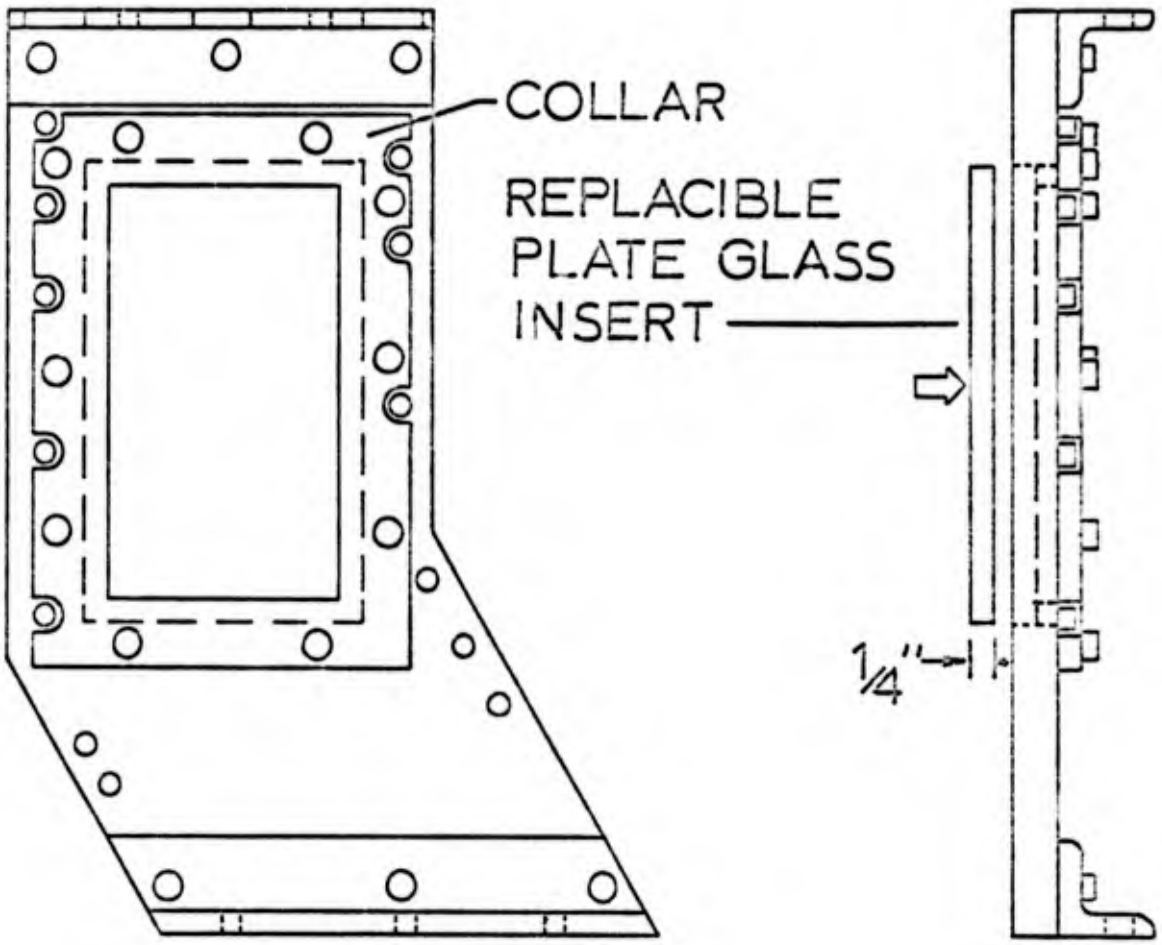

FIG. 3 TEST SECTION PHOTOGRAPHIC INSERT
EROSION RESEARCH FACILITY

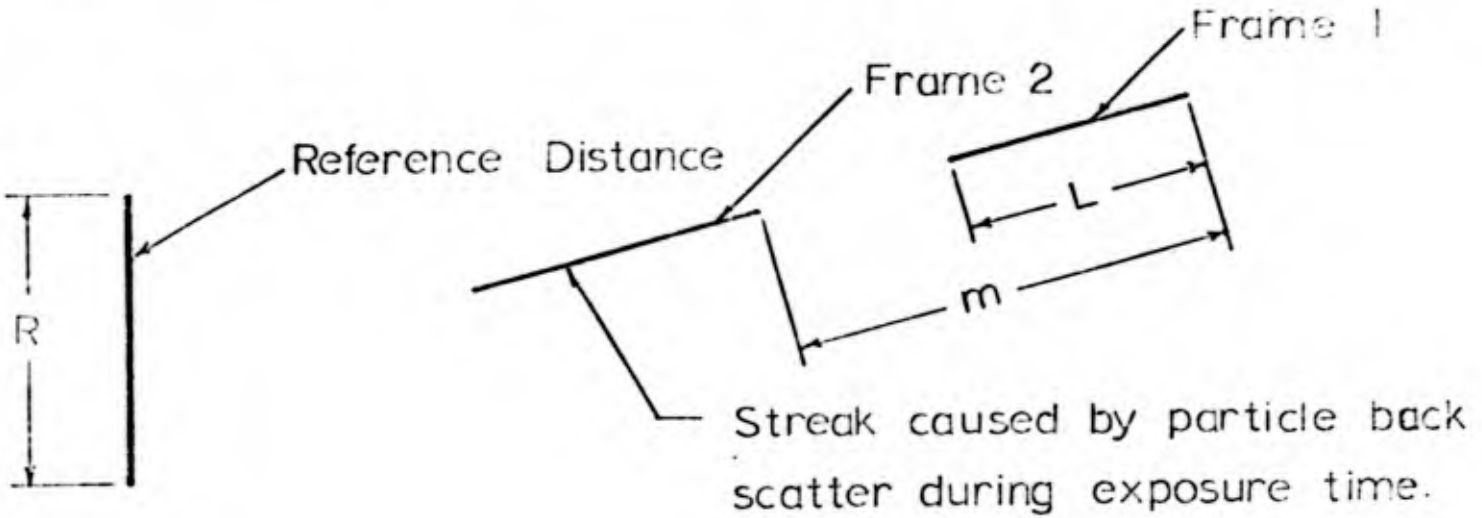

Nomenclature

R - Reference line projected on screen
r - Actual length of reference line
L - Length of particle streak on screen
m - Length traveled by particle between two successive frames
v - Actual velocity of particle
s - Film speed (local quantity) - pictures/second
t_e - Exposure time of frame being observed

FIG 4 HIGH SPEED PARTICLE VELOCITY DATA REDUCTION TECHNIQUE

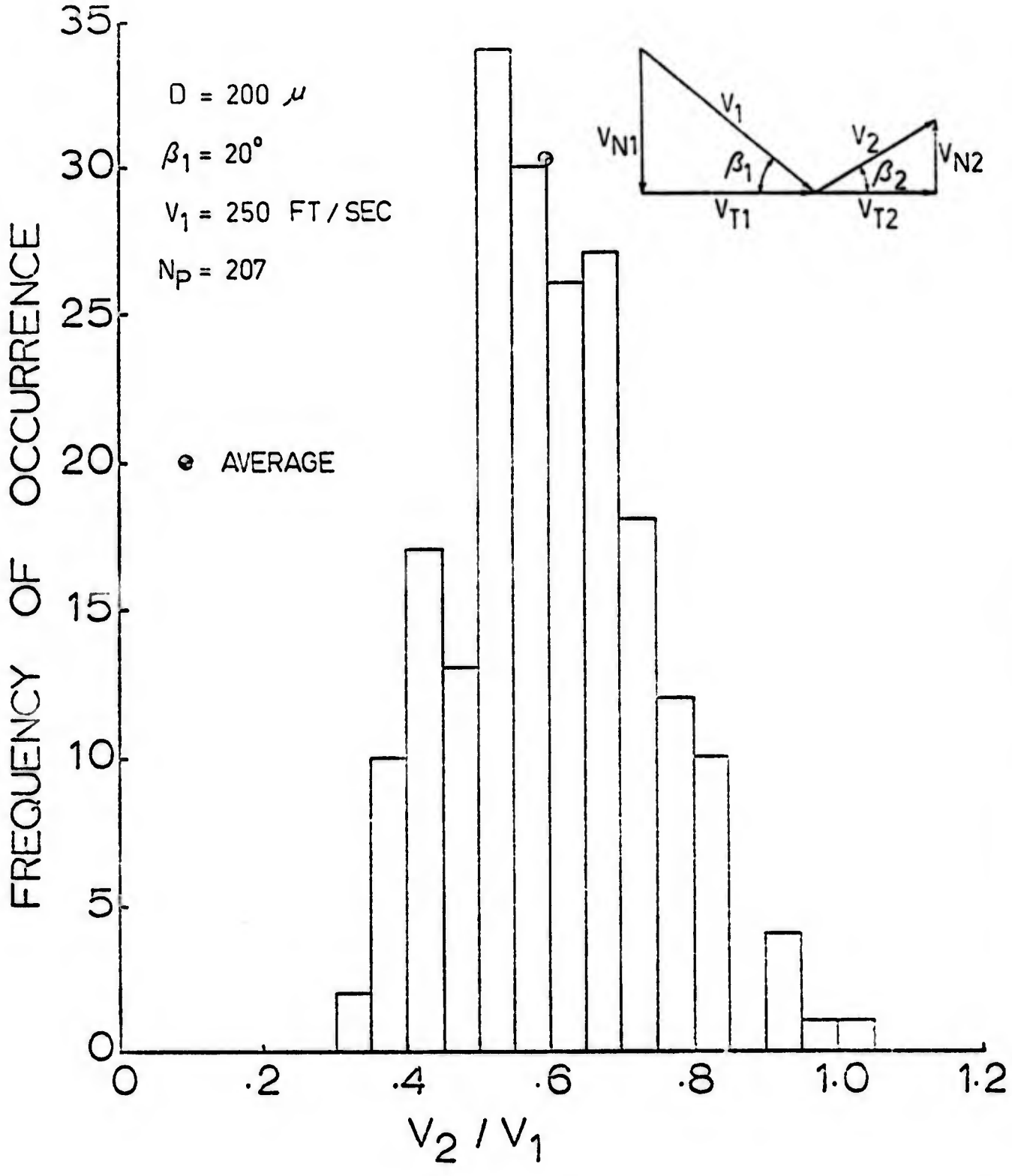

FIG. 5 EROSIVE PARTICLE VELOCITY RESTITUTION RATIO DISTRIBUTION

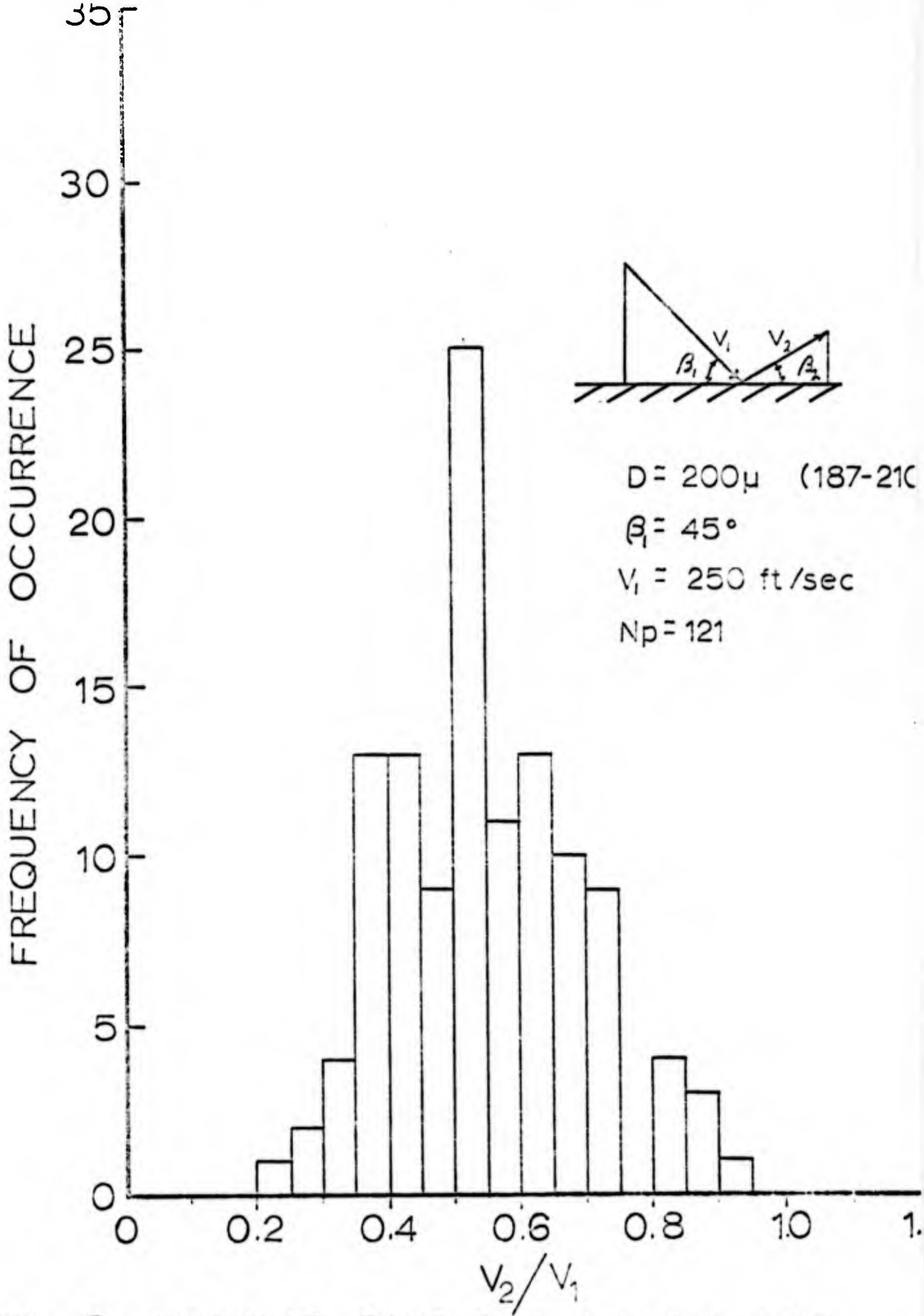

FIG 3 EROSIVE PARTICLE RESTITUTION RATIO DISTRIBUTION

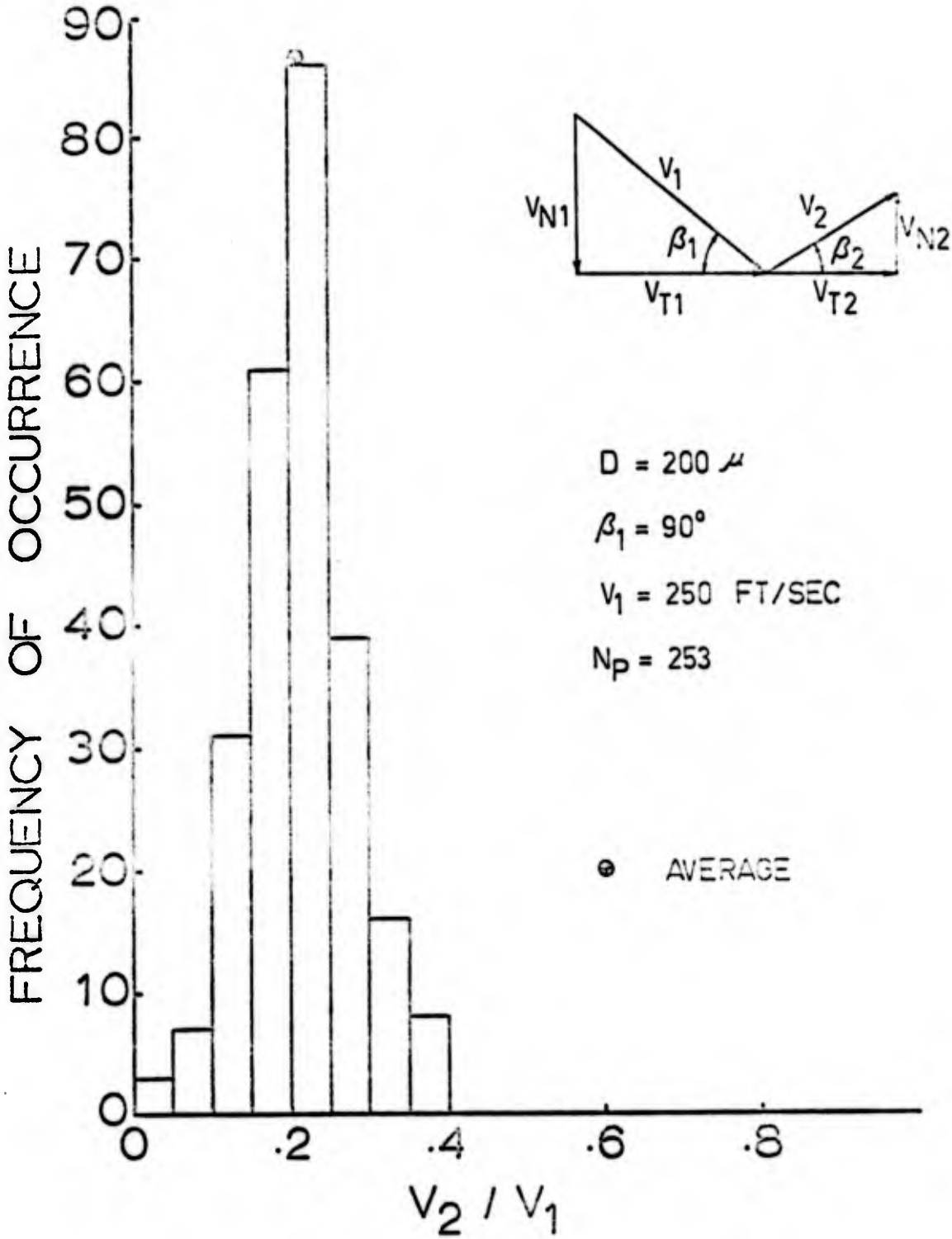

FIG. 7 EROSIVE PARTICLE VELOCITY RESTITUTION RATIO DISTRIBUTION

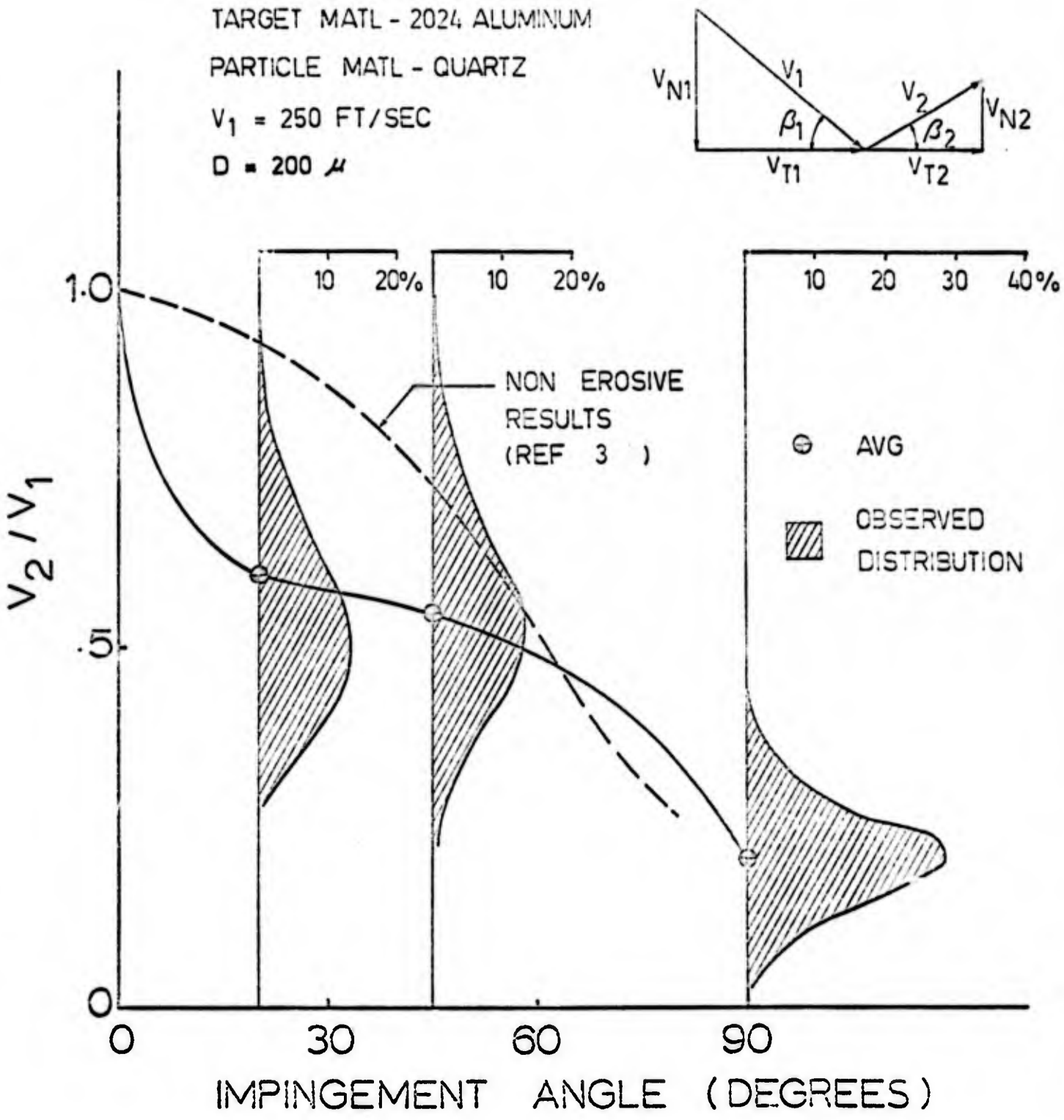

FIG. 8 INFLUENCE OF IMPACT ANGLE ON THE EROSIVE PARTICLE VELOCITY RESTITUTION RATIO

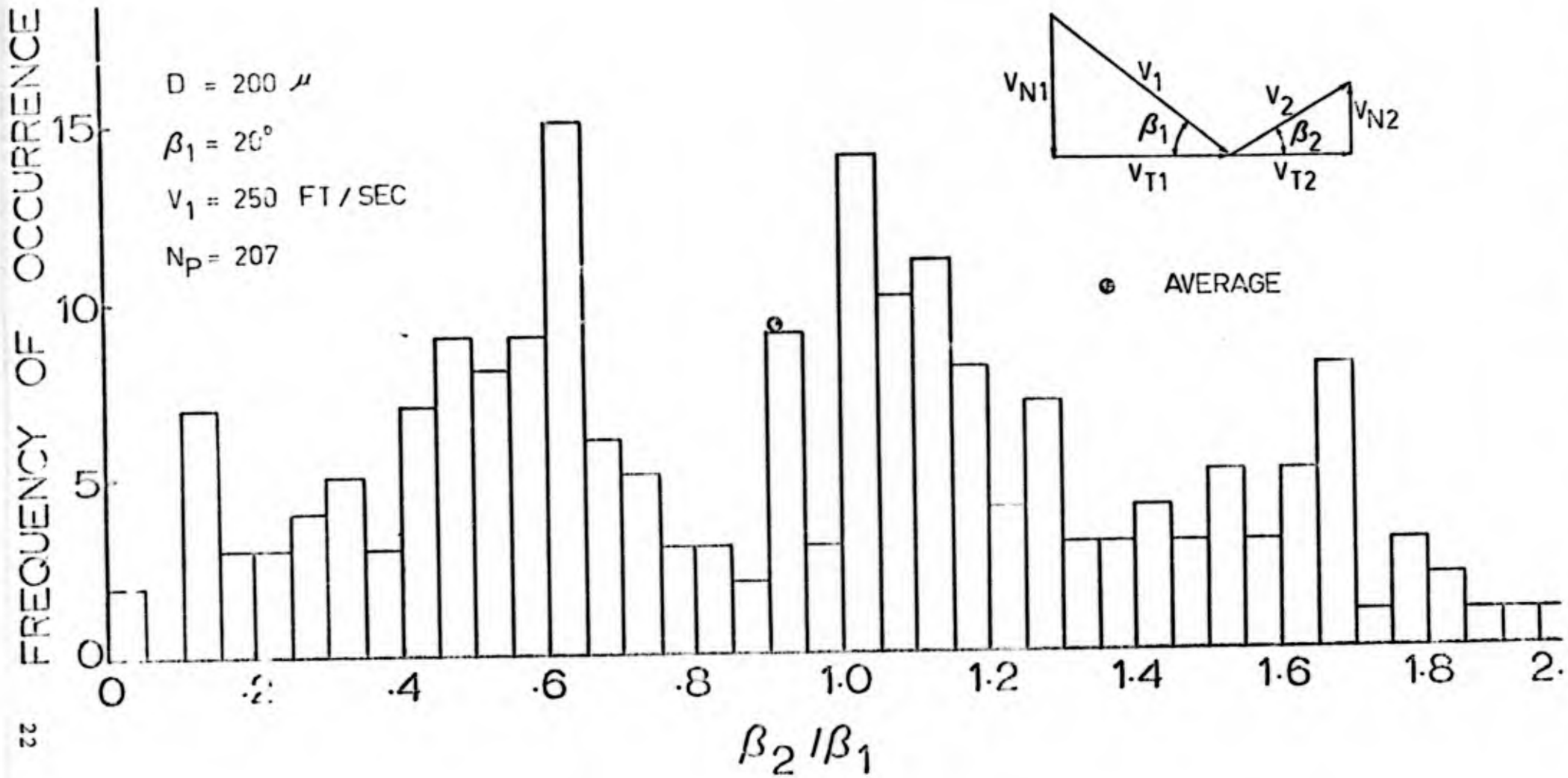

FIG. 9 EROSIVE PARTICLE DIRECTIONAL COEFFICIENT DISTRIBUTION

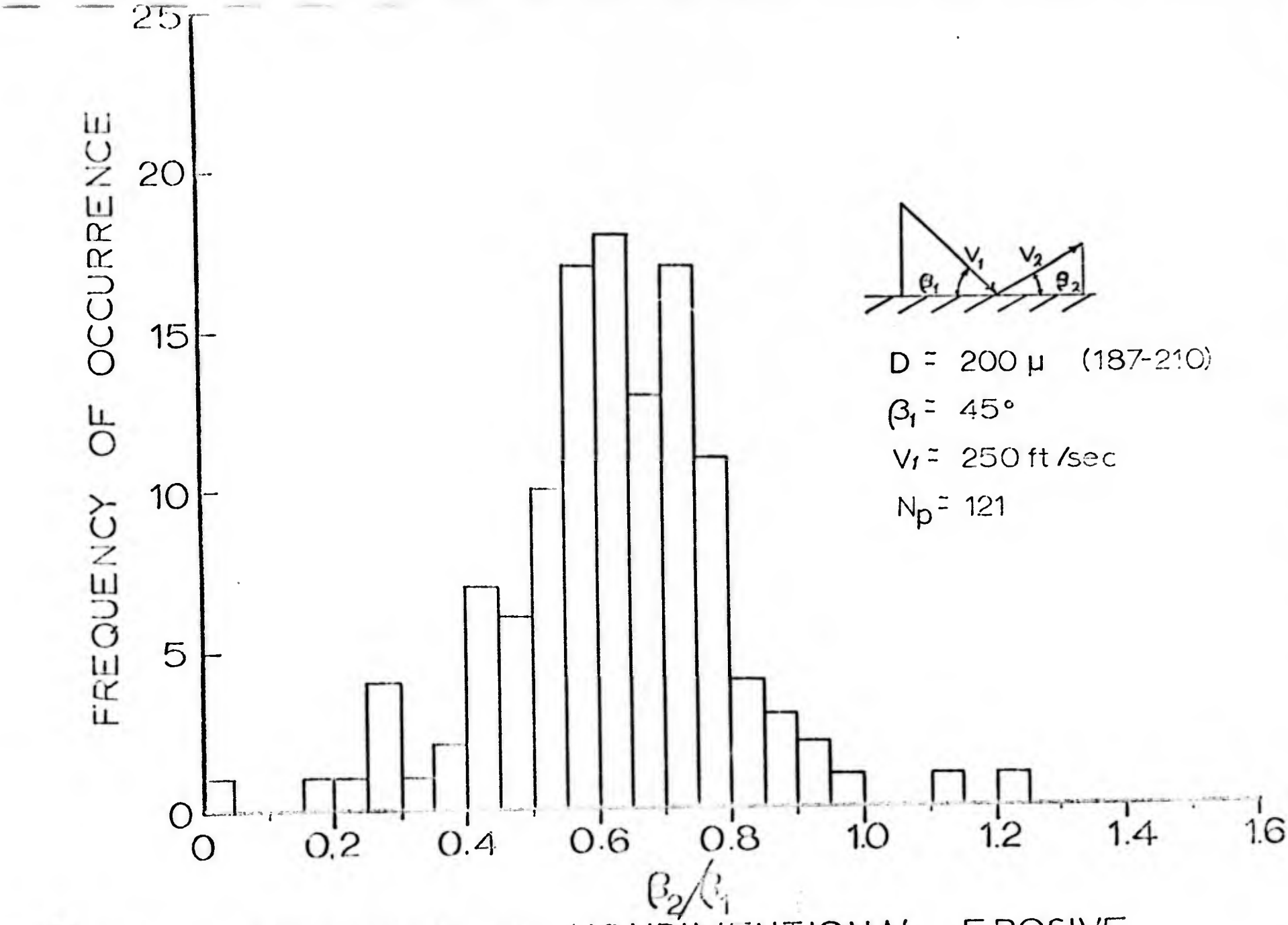

FIG 10 DISTRIBUTION OF NONDIMENTIONAL EROSIVE PARTICLE REBOUND ANGLE

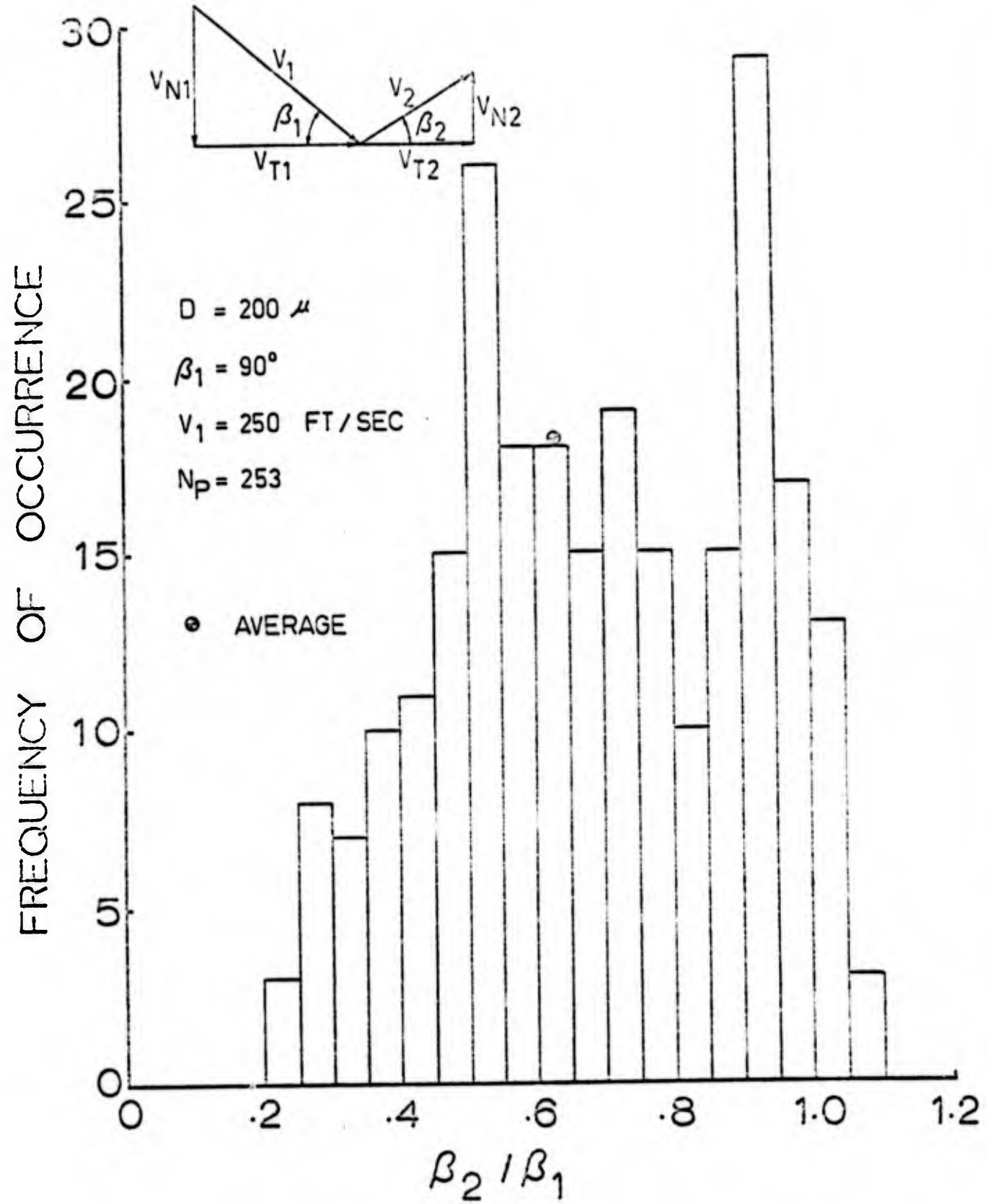

FIG. 11 EROSIVE PARTICLE DIRECTIONAL COEFFICIENT DISTRIBUTION

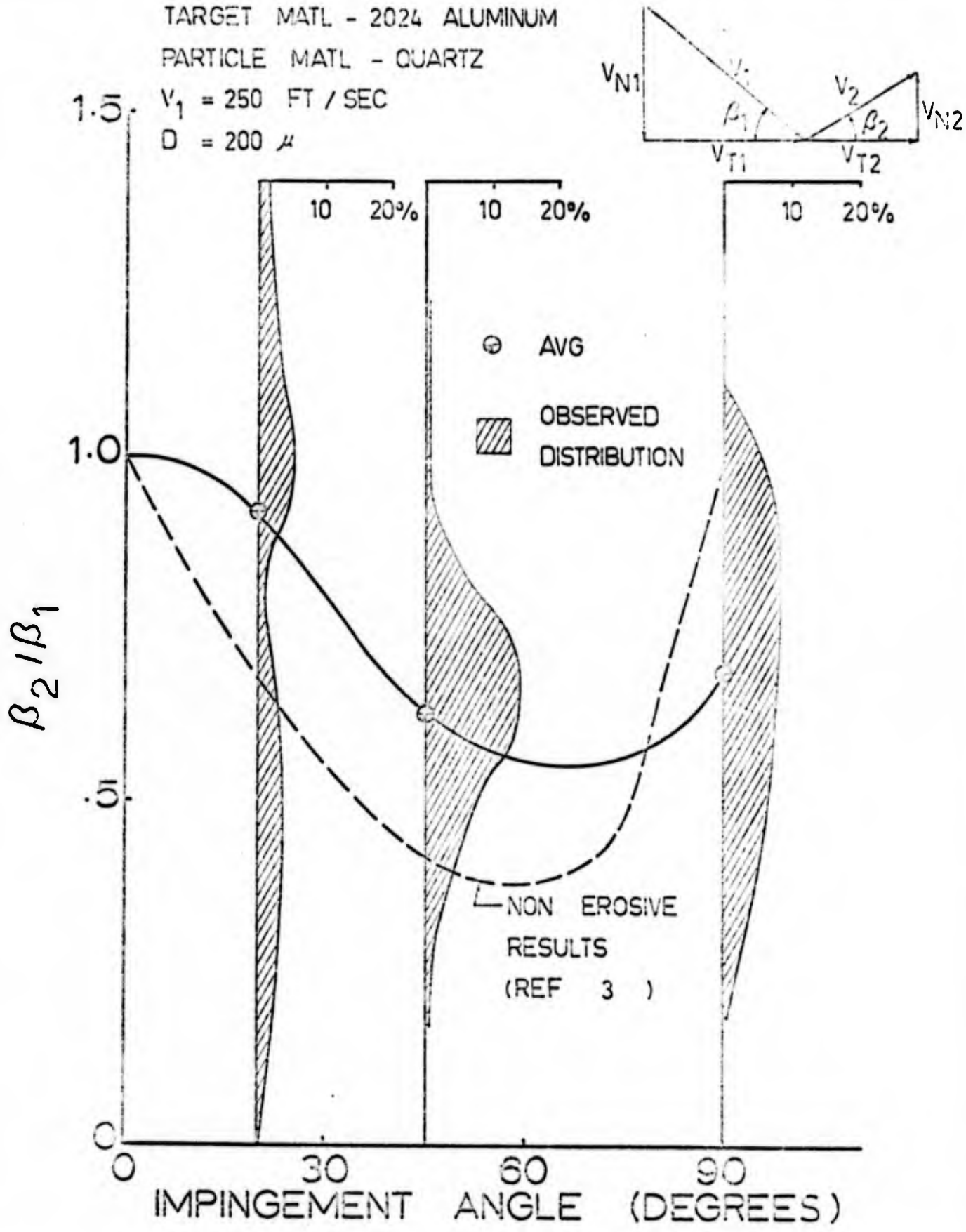

FIG. 12 INFLUENCE OF IMPACT ANGLE ON THE EROSIVE PARTICLE DIRECTIONAL COEFFICIENT

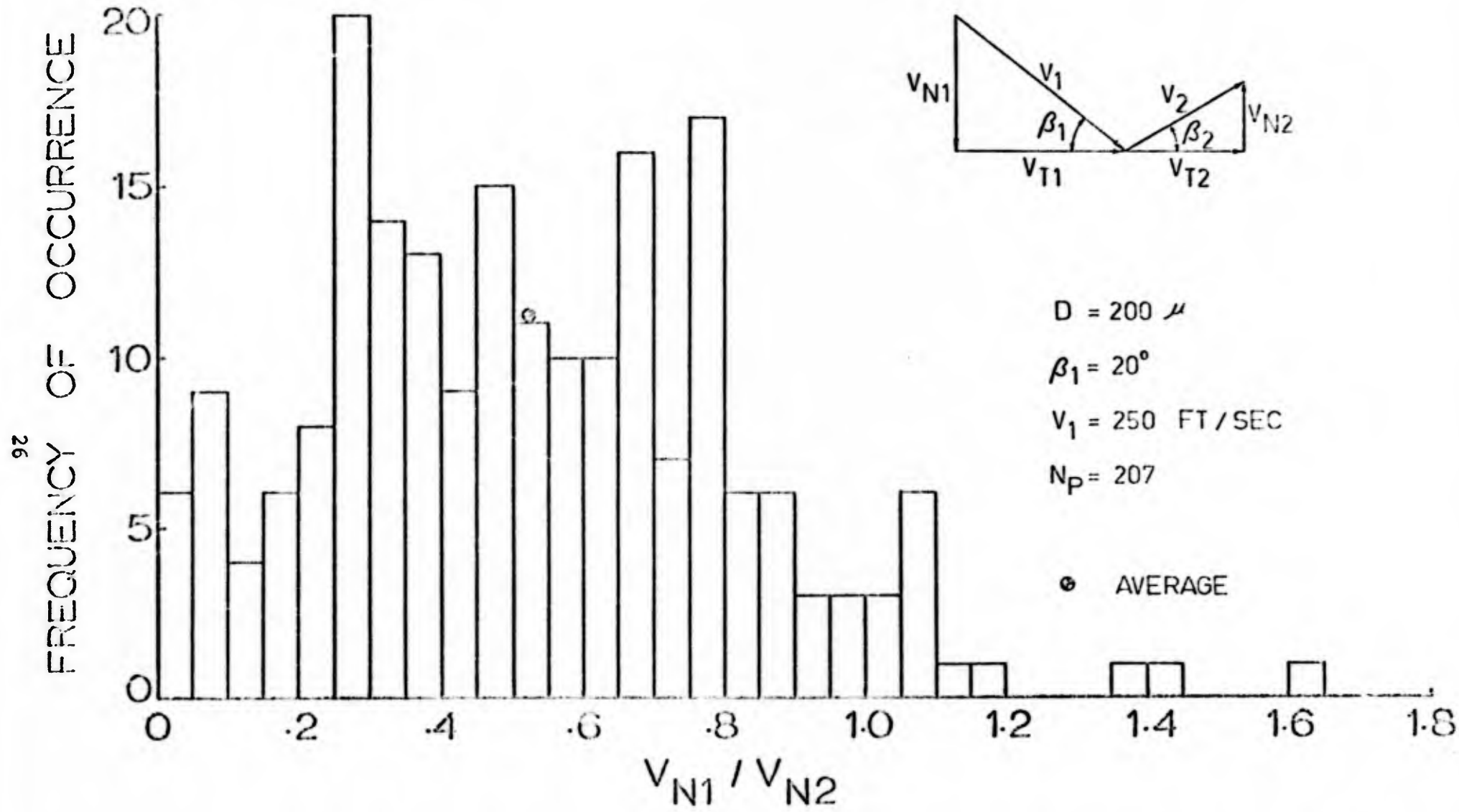

FIG. 13 EROSIVE PARTICLE NORMAL VELOCITY RESTITUTION RATIO DISTRIBUTION

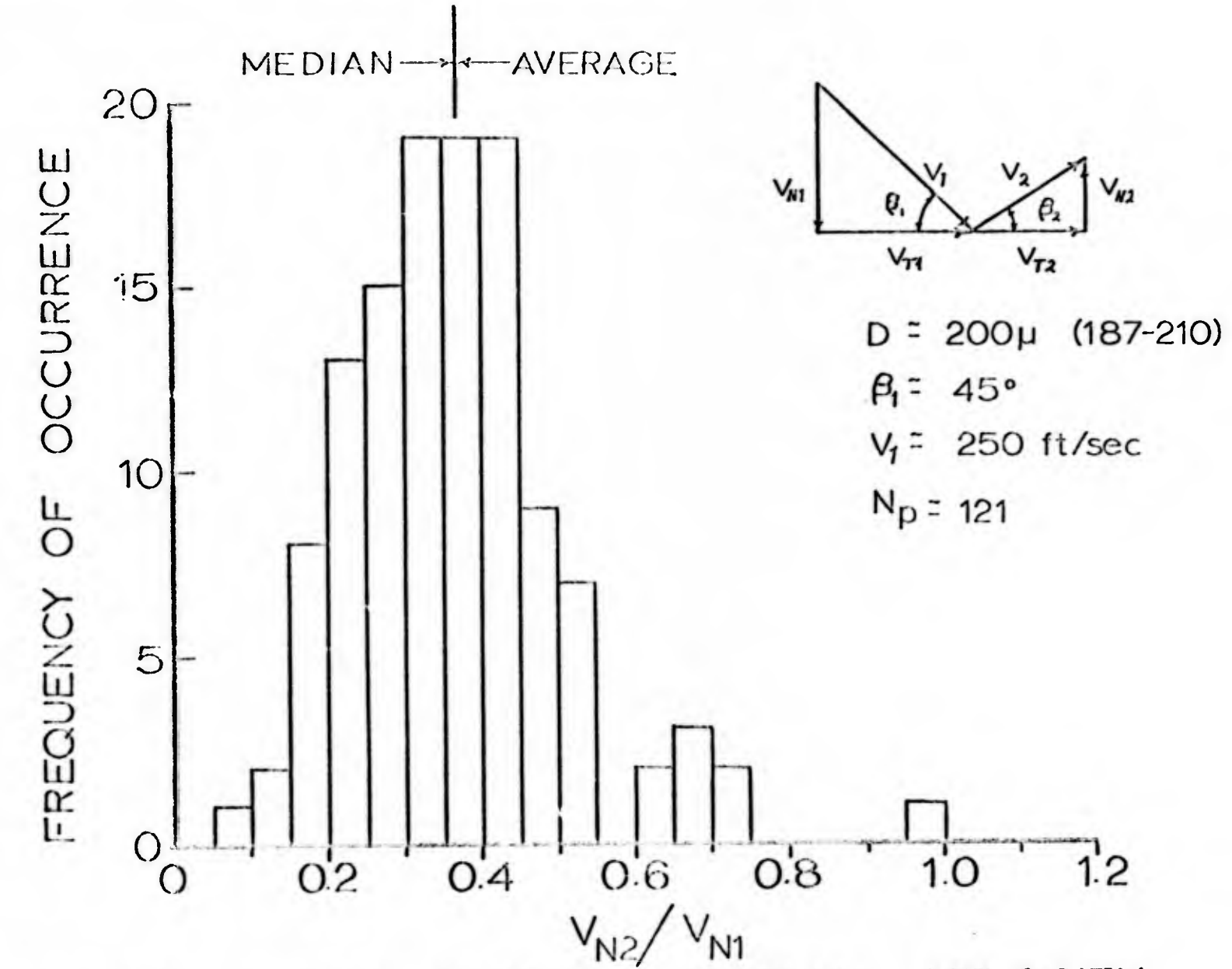

FIG 14 EROSIVE PARTICLE NORMAL VELOCITY RESTITUTION RATIO DISTRIBUTION

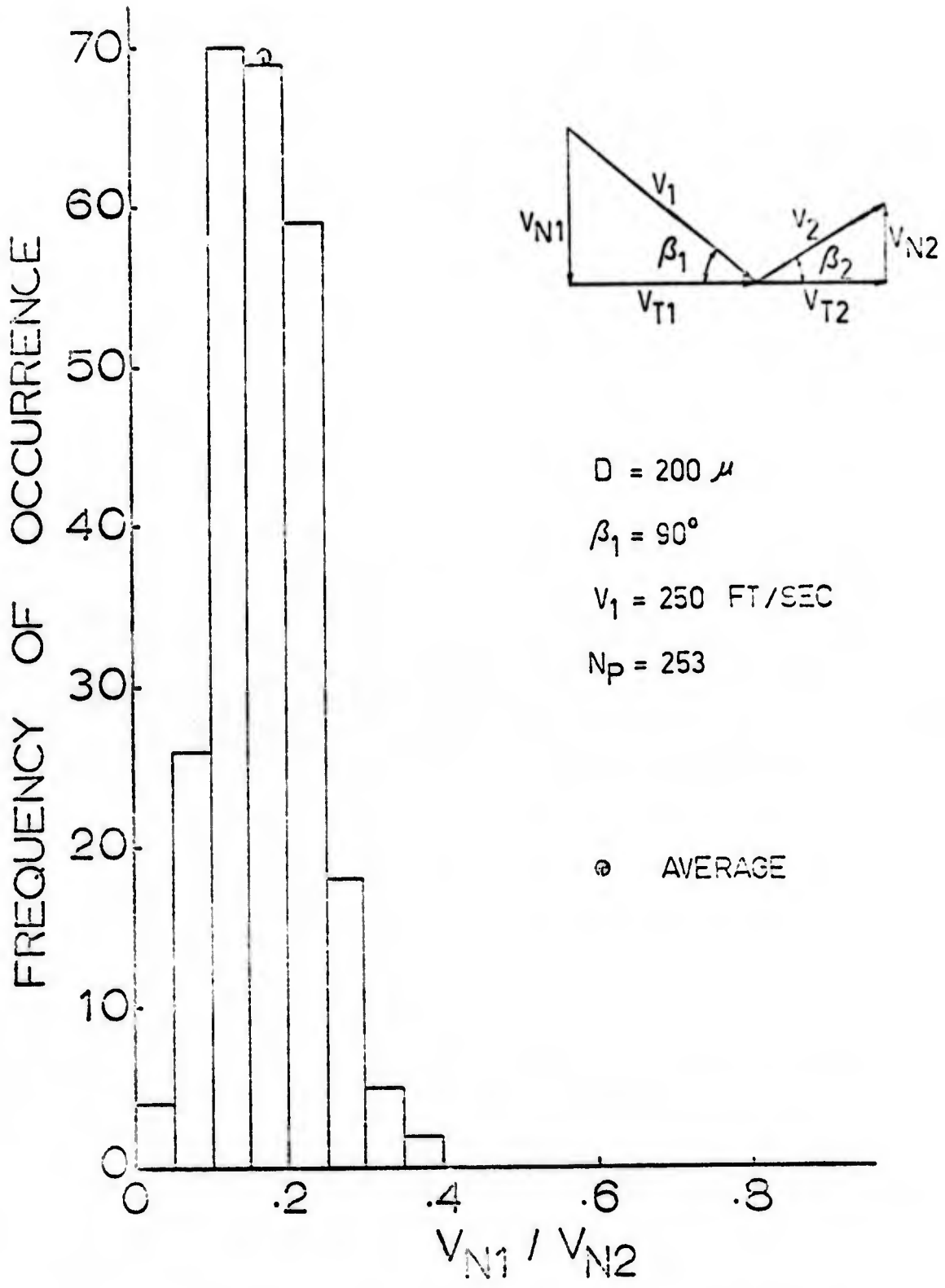

FIG. 15 EROSIVE PARTICLE NORMAL VELOCITY RESTITUTION RATIO DISTRIBUTION

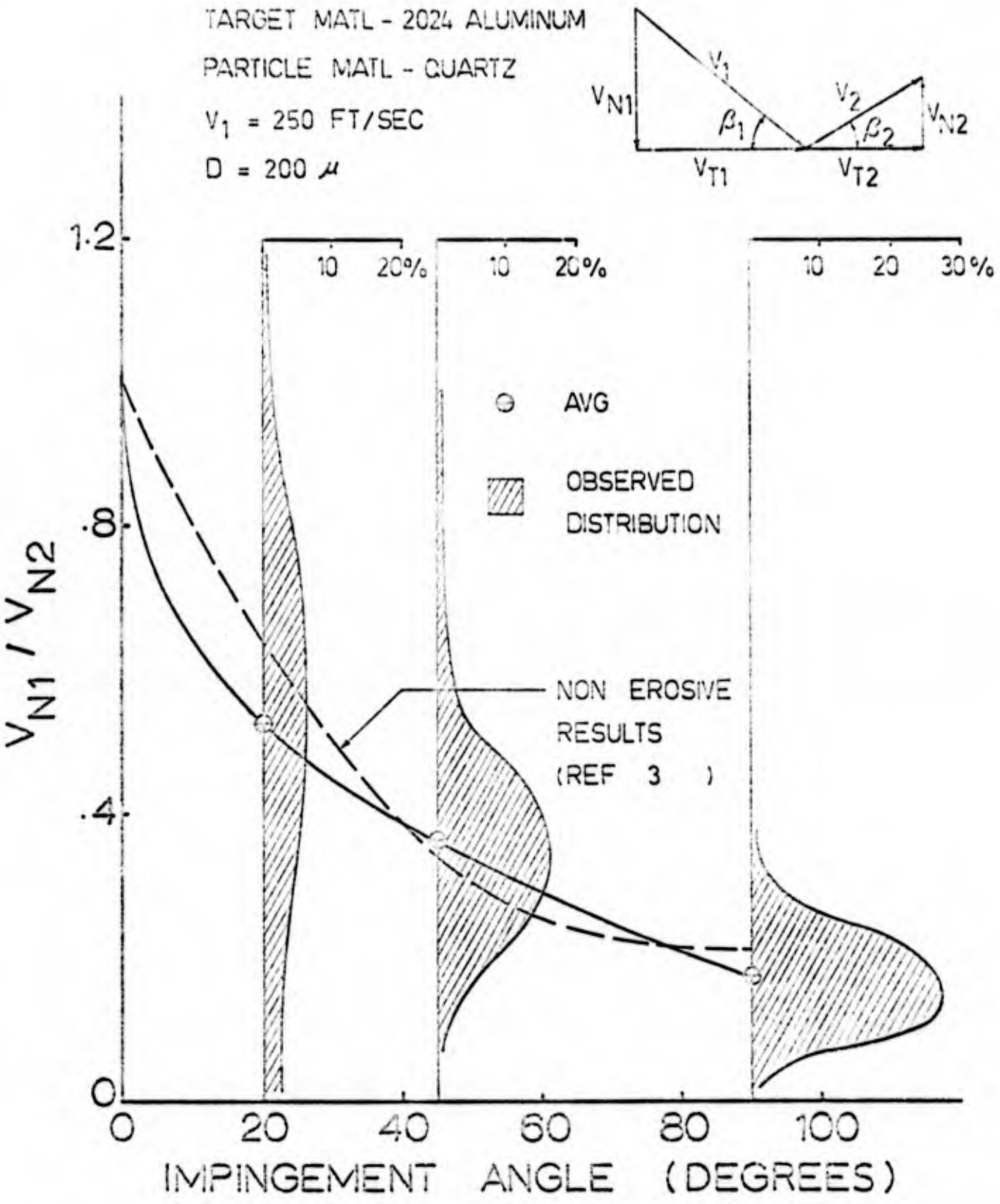

FIG. 16 INFLUENCE OF IMPACT ANGLE ON THE EROSIVE PARTICLE NORMAL VELOCITY RESTITUTION RATIO

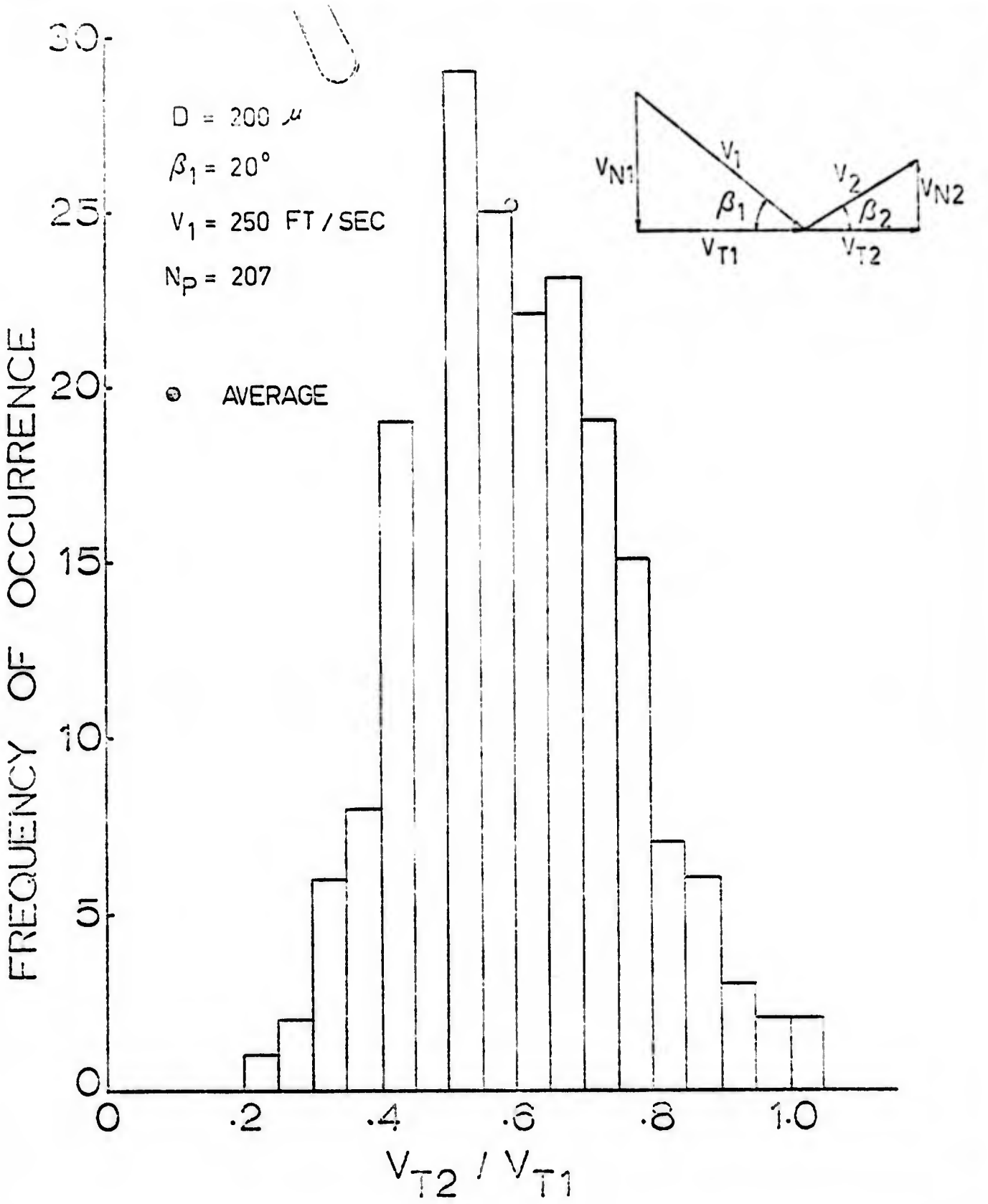

FIG. 17 EROSIVE PARTICLE TANGENTIAL VELOCITY RESTITUTION COEFFICIENT DISTRIBUTION

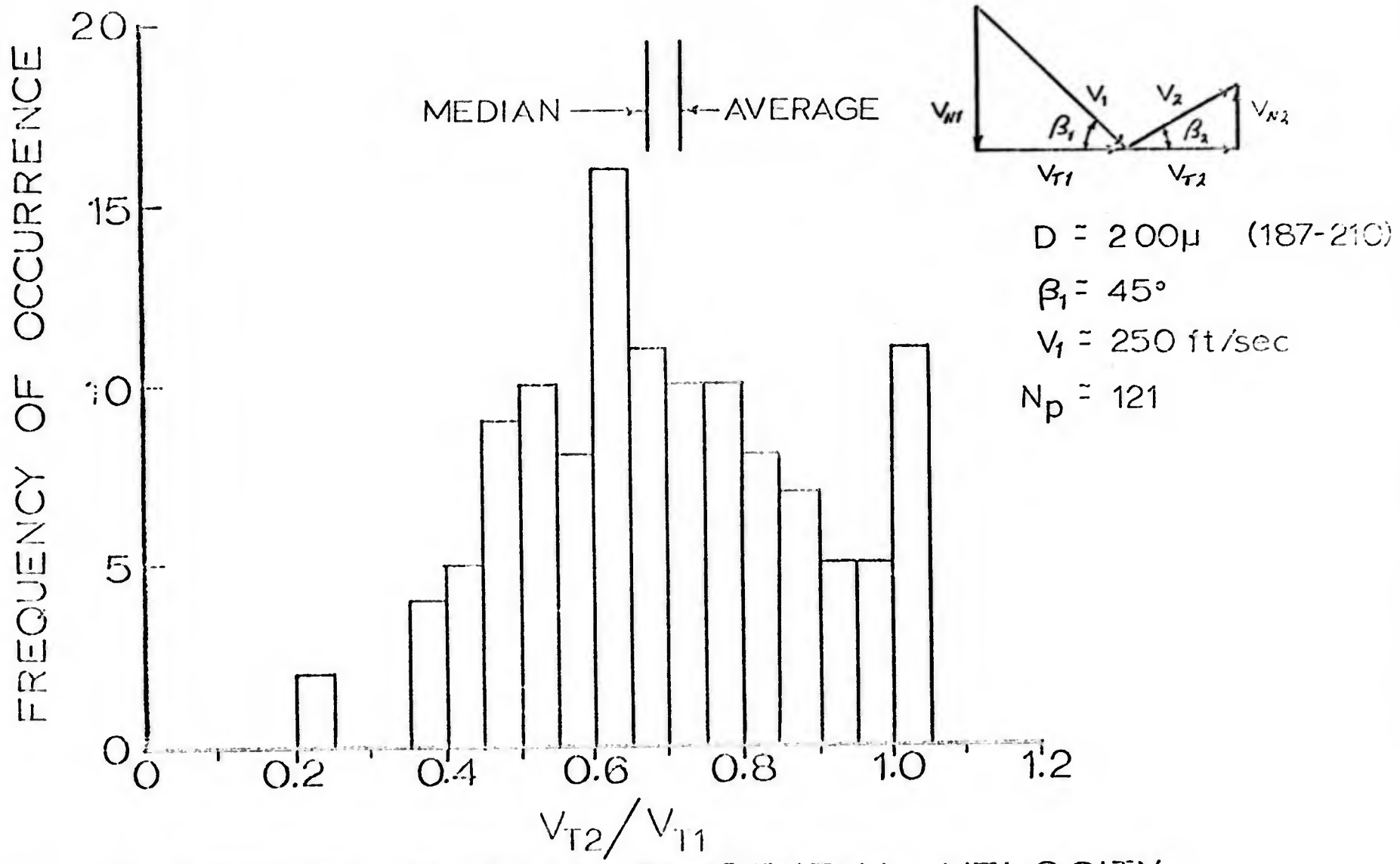

FIG 18 EROSIVE PARTICLE TANGENTIAL VELOCITY RESTITUTION RATIO DISTRIBUTION

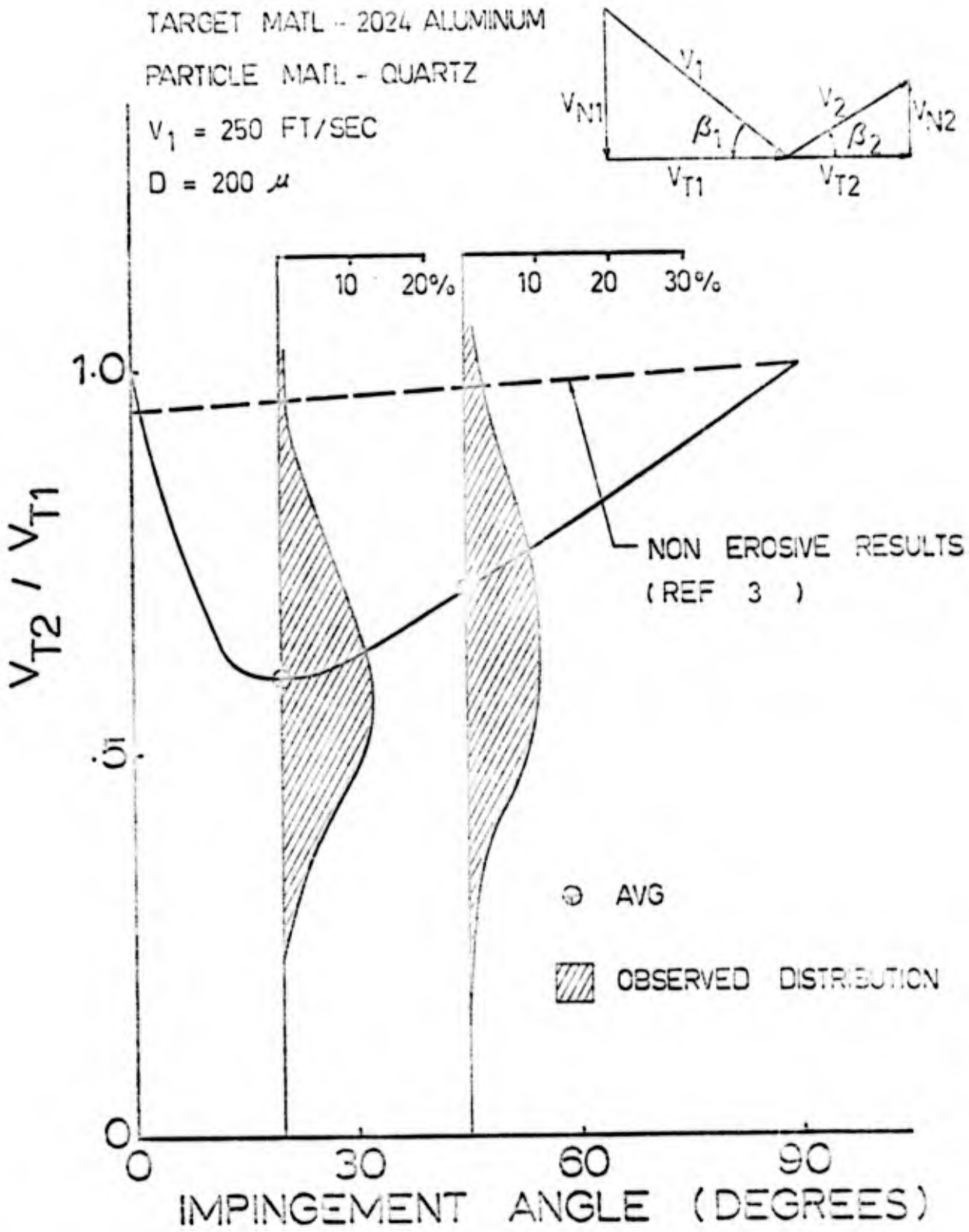

FIG. 19 INFLUENCE OF IMPACT ANGLE ON THE EROSIVE PARTICLE TANGENTIAL VELOCITY RESTITUTION RATIO

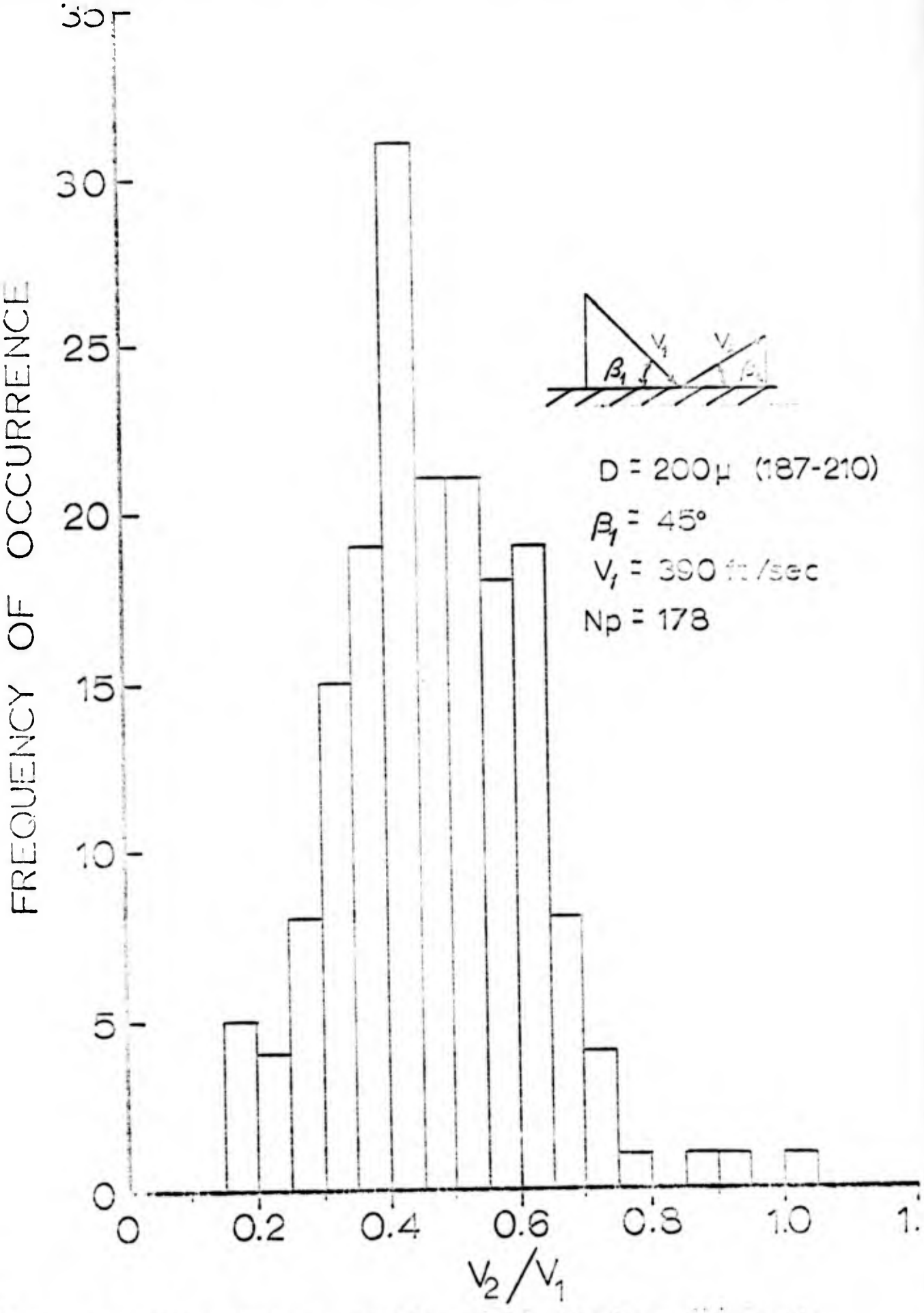

FIG 20 EROSIVE PARTICLE RESTITUTION RATIO DISTRIBUTION

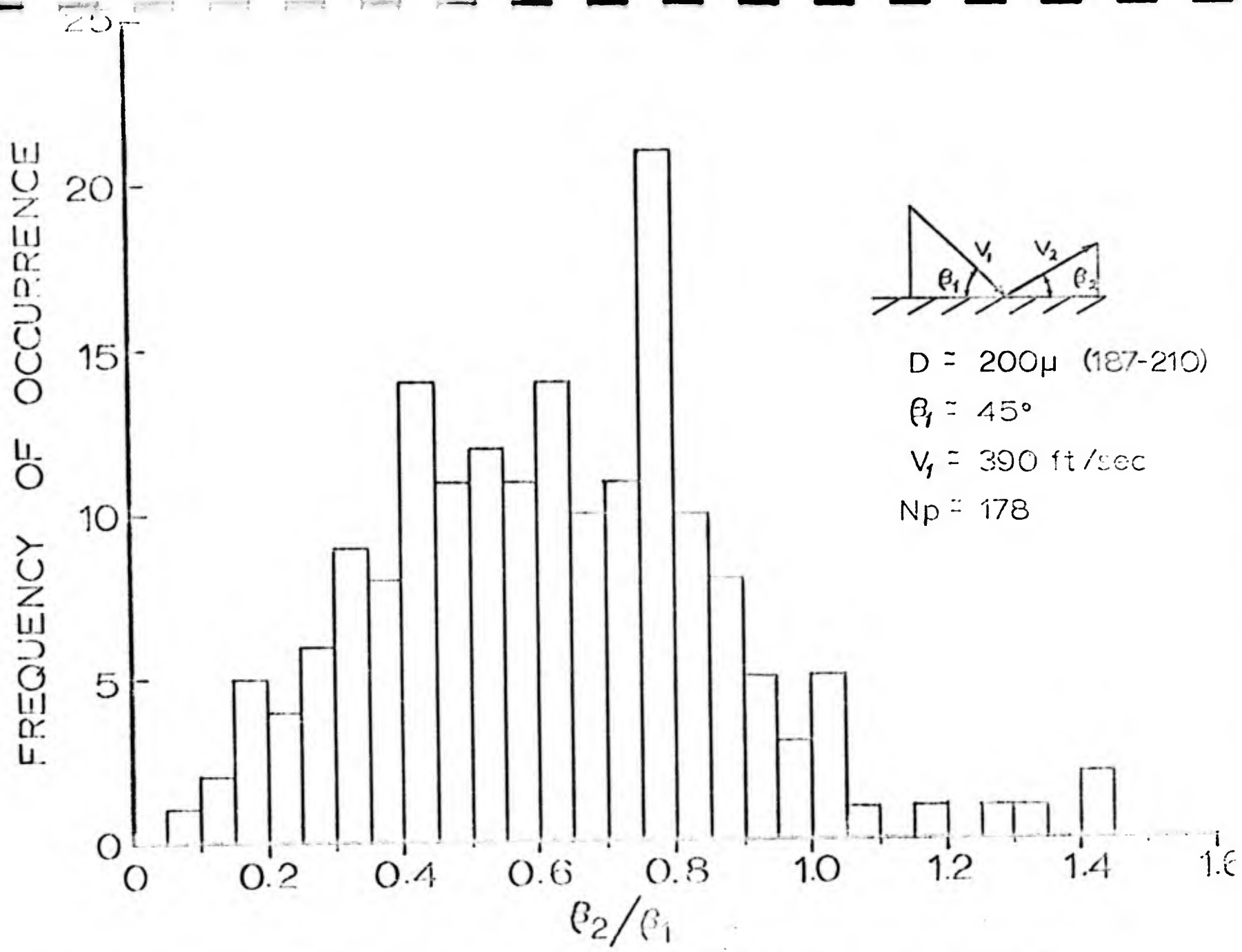

FIG 21 DISTRIBUTION OF NONDIMENTIONAL EROSIVE PARTICLE REBOUND ANGLE

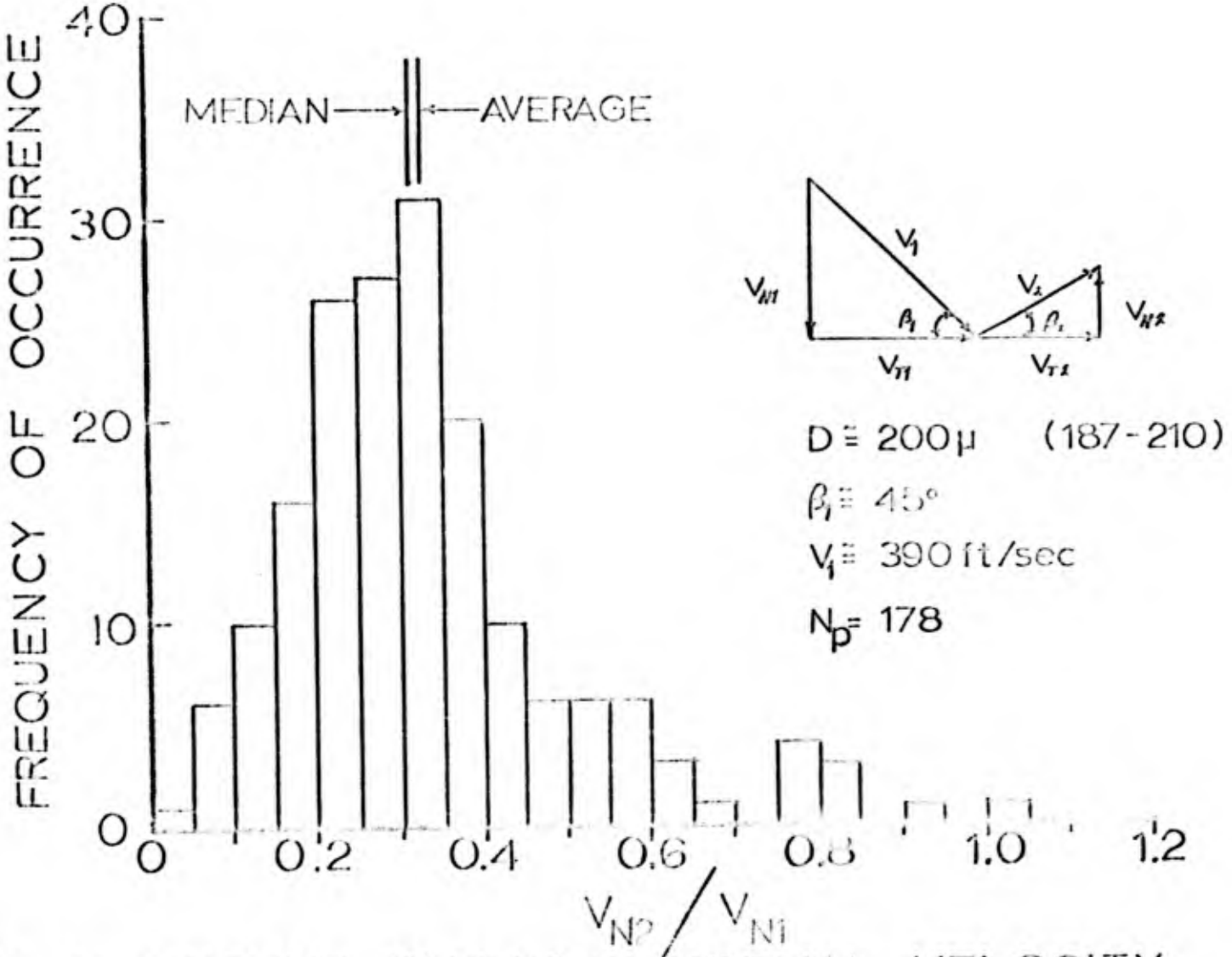

FIG. 22 EROSIVE PARTICLE NORMAL VELOCITY RESTITUTION RATIO DISTRIBUTION

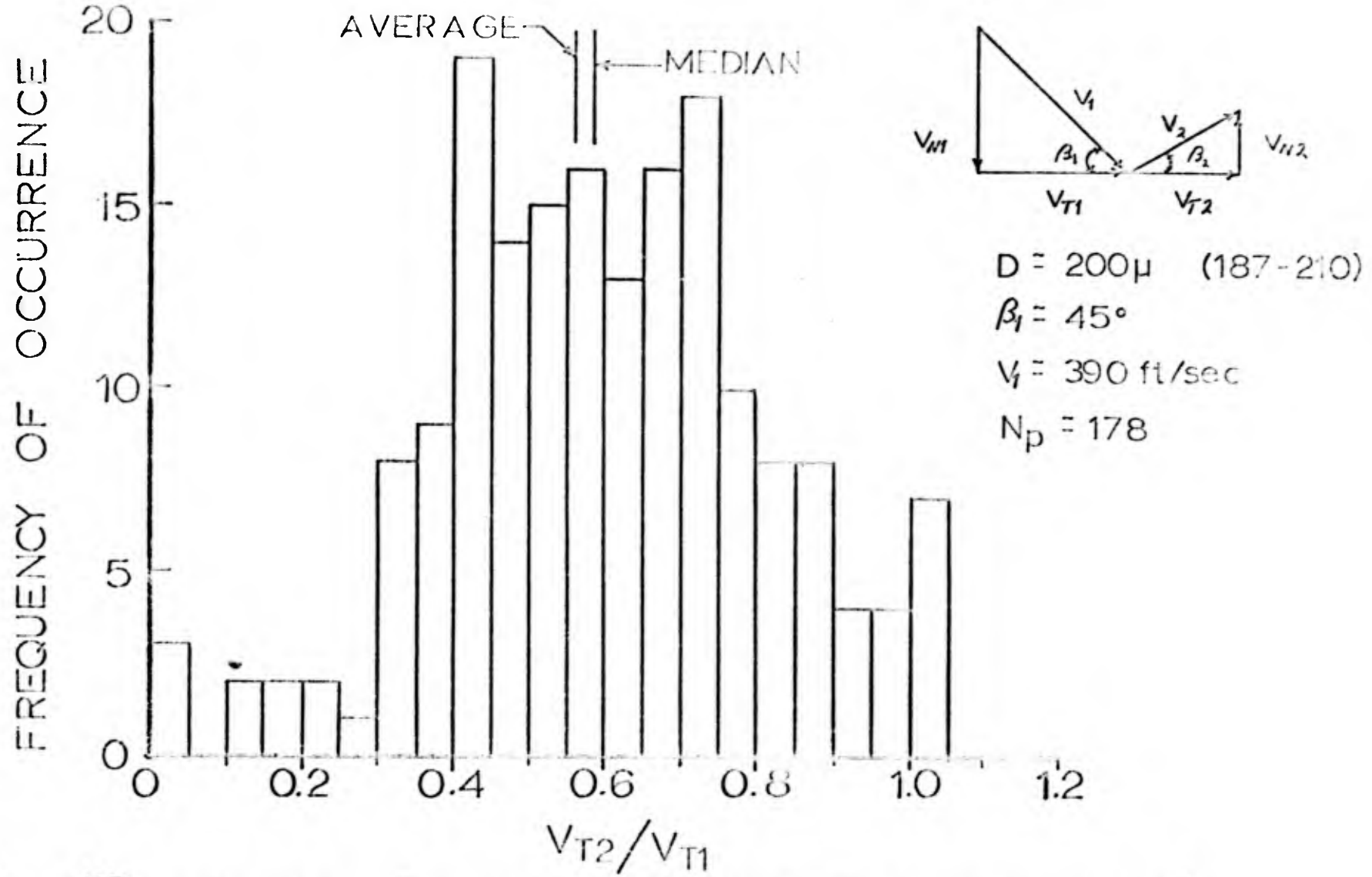

FIG 23 EROSIVE PARTICLE TANGENTIAL VELOCITY RESTITUTION RATIO DISTRIBUTION

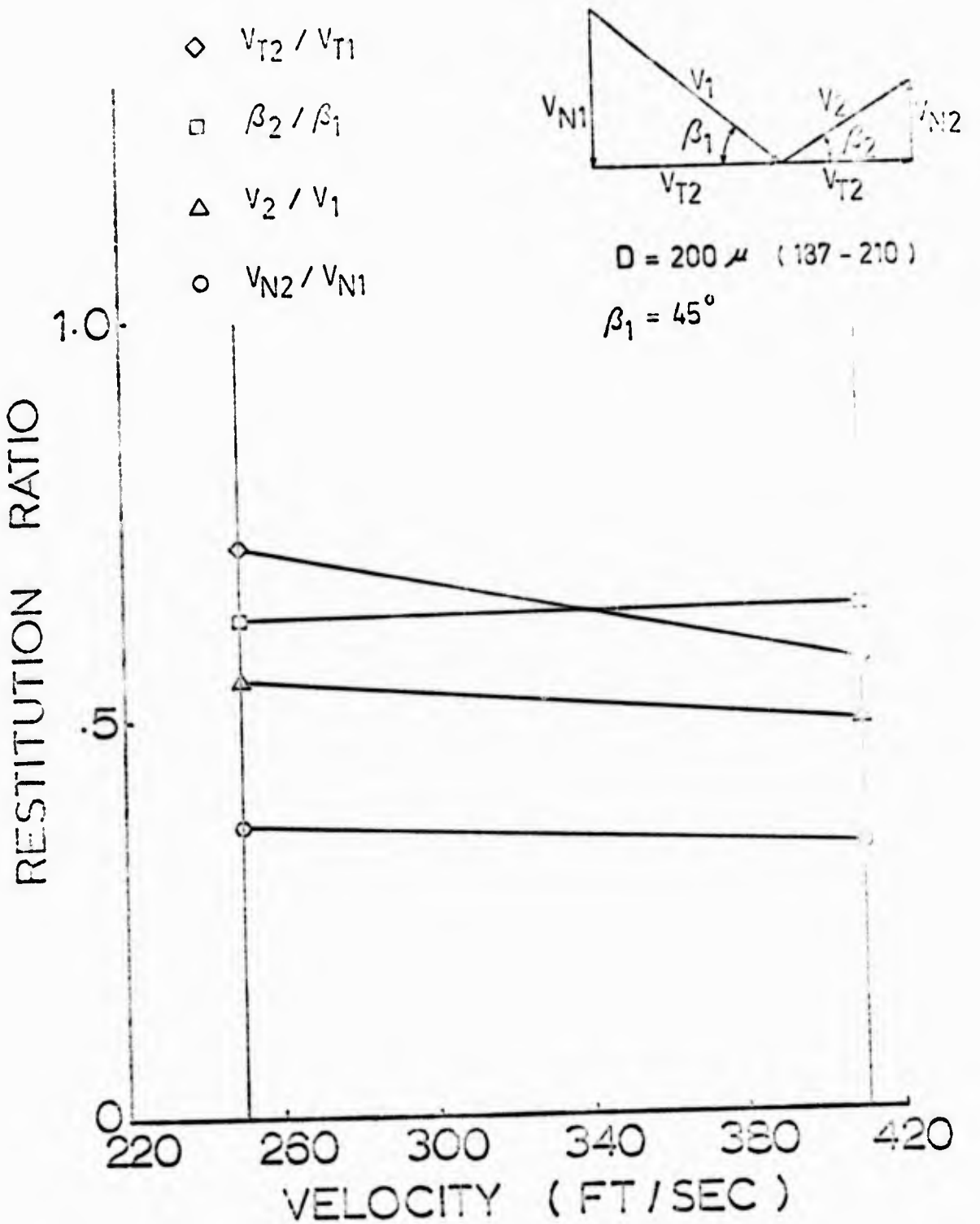

FIG. 24 VELOCITY INFLUENCE ON RESTITUTION RATIO

REFERENCES

1. D. Tabor, "The Hardness of Metals," 1st Edition, Clarendon Press, Oxford, 1951.

2. W. J. Head, "The Development of a Model to Predict the Erosion of Materials by Natural Contaminants," Ph.D. Thesis, Purdue University, 1970.

3. M.F. Hussein and W. Tabakoff, "Calculation of Particle Trajectories in a Stationary Two Dimensional Cascade," Project Themis Report No. 72-27, University of Cincinnati, June 1972.

4. J.H. Neilsonand A. Gilchrist, "Erosion by a Stream of Solid Particles," Wear, 11 (1968) 111-122.

5. I. Finnie, "An Experimental Study on Erosion," Proceedings of the Society for Experimental Stress Analysis, Vol. XVII No. 2, 65-70.

6. G. Grant and W. Tabakoff, "An Experimental Study of Certain Aerodynamic Effects on Erosion," Project Themis Report No. 72-28, University of Cincinnati, July 1972.

7. I. Finnie and Y.H. Kabil, "On the Formation of Surface Ripples During Erosion," Wear, 8 (1965), 60-69.

8. I. Finnie, "The Mechanism of Erosion of Ductile Metals," 1958 Proceedings of Applied Mechanics (ASME), 527-532.

9. C.E. Smeltzer, M.E. Gulden, S.S. McElmury, W.A. Compton, "Mechanics of Sand and Dust Erosion in Gas Turbine Engines," USAAVLABS Technical Report 70-36, August 1970.

10. G.P. Tilly and W. Sage, "The Interaction of Particle and Material Behavior in Erosion Processes," Wear, 16 (1970) 447.

11. G.L. Sheldon, "Similarity and Differences in the Erosion Behavior of Materials," J. Basic Engineering (Trans. ASME Ser. D), 92 (1970) 619.

12. J.E. Goodwin, W. Sage, G.P. Tilly, "A Study of Erosion by Solid Particles," Proc. Inst. Mech. Engrs. 184 (15) (1969) 279.

13. I. Finnie, J. Wolak and Y. Kabil, "Erosion of Metals by Solid Particles," J. Mater. 2 (3) (1967) 682.

14. G.L. Sheldon and Ashok Kanbere, "An Investigation of Impingement Erosion Using Single Particles," Wear, 21 (1972) 195.